Published in final edited form as:
Nature. 2018 October ; 562(7728): 595–599. doi:10.1038/s41586-018-0581-5.

Otx2 restricts entry to the mouse germline

Jingchao Zhang[#1], **Man Zhang**[#1], **Dario Acampora**[2], **Matúš Vojtek**[1], **Detian Yuan**[3], **Antonio Simeone**[2], and **Ian Chambers**[1]

[1]MRC Centre for Regenerative Medicine, Institute for Stem Cell Research, School of Biological Sciences, University of Edinburgh, 5 Little France Drive, Edinburgh EH16 4UU, Scotland [2]Institute of Genetics and Biophysics "Adriano Buzzati-Traverso", CNR, Via P. Castellino, 111, 80131 Naples, Italy [3]Department of Biochemistry and Molecular Biology, Shandong University School of Medicine, Jinan, 250012, PR China

[#] These authors contributed equally to this work.

Summary

The successful segregation of germ cells from somatic lineages is vital for sexual reproduction and species survival. In the mouse, primordial germ cells (PGCs), precursors of all germ cells, are induced from the post-implantation epiblast1. Induction requires BMP4 signalling to prospective PGCs2 and the intrinsic action of PGC transcription factors (TFs)3–6. However, the molecular mechanisms connecting BMP4 to induction of the PGC TFs responsible for segregating PGCs from somatic lineages are unknown. Here we show that the transcription factor OTX2 is a key regulator of these processes. Down-regulation of *Otx2* precedes the initiation of the PGC programme both *in vitro* and *in vivo*. Deletion of *Otx2* in vitro dramatically increases PGCLC differentiation efficiency and prolongs the period of PGC competence. In the absence of Otx2 activity, PGCLC differentiation becomes independent of the otherwise essential cytokine signals, with germline entry initiating even in the absence of the PGC TF Blimp1. Deletion of *Otx2* in vivo increases PGC numbers. These data demonstrate that OTX2 functions repressively upstream of PGC TFs, acting as a roadblock to limit entry of epiblast cells to the germline to a small window in space and time, thereby ensuring correct numerical segregation of germline cells from the soma.

Different species form their germ cells by either of two general methods: segregation of preformed germplasm, or induction by signalling 7,8. In mammals, germ cell precursors

Correspondence and requests for materials should be addressed to ichambers@ed.ac.uk; mzhang33@ed.ac.uk.

Data Availability

All the datasets generated or analysed during the current study are available from the corresponding author on reasonable request.

Author Contributions

JZ, MZ and IC conceived the project and designed experiments. AS and DA provided reagents and advice. DY performed bioinformatics analysis. JZ and MZ performed experiments, with help from MV. JZ, MZ and IC analysed the data. IC wrote the paper with input from all authors.

Author Information

Reprints and permissions information is available at www.nature.com/reprints.

The authors declare no competing financial interests.

Europe PMC Funders Author Manuscripts

arise by induction 9–11. In the mouse, competence to initiate germ cell development is restricted to a few cells within the E5.5-6.25 epiblast 1. BMP4 from the extraembryonic ectoderm acts on these competent cells to specify germ cell identity 2. Specification also requires transcription factors (TFs), notably Blimp1, Ap2γ and Prdm14 3–6. However, the molecular mechanisms connecting exposure of competent cells to BMP4 to activation of PGC TFs are obscured by limited access to the peri-implantation embryo. Recently, a system for differentiation of primordial germ cell-like cells (PGCLCs) from embryonic stem cells (ESCs) via germline competent epiblast-like cells (EpiLCs) 12 has opened up investigation of molecular events segregating germline and soma.

During the ESC to EpiLC transition the TF OTX2 becomes expressed and redirects binding of OCT4 to genomic regulatory elements13,14. OTX2 was previously characterised as a regulator of anterior patterning 15,16. Recent work has demonstrated antagonistic functions for OTX2 and NANOG in ESCs17,18. A positive role for NANOG in PGCLC differentiation has also been added to the known requirements for Blimp1, Prdm14 and Ap2γ 19–21. We therefore assessed expression of the corresponding mRNAs following addition of PGCLC-inducing cytokines to EpiLCs (Figure 1a, b). *Blimp1*, *Prdm14* and *AP2γ* mRNAs did not change during the first 12 hours. A modest increase in *Ap2γ* mRNA at 24h preceded more pronounced increases in all three mRNAs by 48h (Figure 1b). In contrast, *Otx2* mRNA dropped to ~20% of the EpiLC level at 24h (Figure 1b). Immunofluorescence analysis indicated that the proportion of cells expressing OTX2 protein decreased at 24h, with almost no OTX2-expressing cells detected at 48h (Figure 1c; Extended Data Figure 2a, b). Cultures in which PGCLC cytokines were omitted lost OTX2-expressing cells more slowly (Extended Data Figure 2a, b). Moreover, while *Otx2* mRNA declines upon FGF/Activin withdrawal, the kinetics of suppression are enhanced by PGCLC cytokine addition (Extended Data Figure 2d). This suggests that PGCLC cytokines directly repress *Otx2* transcription, a notion supported by the prompt decline in *Otx2* pre-mRNA upon switching EpiLCs into PGCLC media (Extended Data Figure 2e). BLIMP1 and AP2γ proteins were initially detectable at 24h, but only in cultures treated with cytokines (Extended Data Figure 2a, b) and only in cells with reduced OTX2 (Figure 1c, d; Extended Data Figure 2c). These results suggest that before the PGC gene regulatory network (GRN) becomes activated, the transcriptional circuitry of the formative pluripotent 22, germline competent 23 state characterised by OTX2 expression 13 becomes extinguished.

The reciprocal relationship between OTX2 and BLIMP1/AP2γ during PGCLC induction prompted determination of whether a similar spatio-temporal relationship between changes in expression of OTX2 and PGC TFs held *in vivo*. Whole mount immunofluorescence of pre-streak stage embryos indicated that all epiblast cells express both OCT4 and OTX2 (Figure 1e). At early-mid streak, OTX2 remains widely expressed in the epiblast except for cells showing incipient FRAGILIS 24 and BLIMP1 3 expression (Figure 1f, h). By late streak-early bud stage, BLIMP1 is clearly detectable within the FRAGILIS field in cells lacking OTX2 (Figure 1g, i). These results indicate that OTX2 is expressed ubiquitously in pre-streak epiblast cells but is specifically down regulated in the prospective PGC population prior to BLIMP1 expression.

Cytokine addition is required for PGCLC differentiation 12. To assess when, cells were treated for 1, 2 or 6 days with cytokines and analysed by FACS for surface expression of SSEA1 and CD61, which together mark PGCLCs 12. Cytokine treatment for the first day induces around half of the potentially responsive population to become $CD61^+/SSEA1^+$ (Extended Data Figure 2f). Two or 6 days of cytokine treatment were equally effective at inducing CD61/SSEA1 (Extended Data Figure 2f). This suggests that cytokine exposure reaches maximum efficacy at 2 days, the time required to reduce Otx2 to minimal levels and initiate PGCLC TF expression (Figure 1b, d; Extended Data Figure 2a, b, c).

To directly assess whether OTX2 downregulation influences entry of pluripotent cells into the germline, *Otx2*-null cells were examined. A transgenic Oct4ΔPE::GFP reporter activated upon germline entry 25 was added to $Otx2^{fl/-}$ and $Otx2^{-/-}$ ESCs 17(Extended Data Figure 1). Compared to *Otx2* heterozygotes, $Otx2^{-/-}$ cell populations showed widespread activation of Oct4ΔPE, with essentially all cells activating GFP (Figure 2a). Furthermore, the $SSEA1^+/CD61^+$ cell number is increased 5-10-fold in $Otx2^{-/-}$ versus $Otx2^{+/+}$ cells (Figure 2b). This was also the case in independently generated $Otx2^{-/-}$ ESCs (Extended Data Figure 3b) and in additional independent $Otx2^{-/-}$ ESCs generated using CRISPR/Cas9 (Extended Data Figure 1, 3c). Three new ESC lines lacking OTX2 protein (Extended Data Figure 3d) showed enhanced CD61/SSEA1 expression during PGCLC differentiation (Extended Data Figure 3e). These results confirm that a lack of OTX2 promotes germline differentiation.

To investigate when during differentiation OTX2 influences germline entry, an Otx2-ER^{T2} transgene (enabling tamoxifen-induced re-localisation of OTX2) was introduced into $Otx2^{lacZ/GFP}$ ESCs (Figure 2c, Extended Data Figure 4a). Tamoxifen treatment for the first 2 days suppressed emergence of $SSEA1^+/CD61^+$ cells (Figure 2d). These results establish that enforcing OTX2 activity at a time when cells are competent to enter the germline 12 and when cytokines act to decrease endogenous *Otx2* expression, is sufficient to block cytokine-mediated PGCLC differentiation.

To examine the mechanism by which OTX2 inhibits PGCLC differentiation, mRNAs were analysed. Expression of PGCLC TF mRNAs occurred sooner and to a greater extent without OTX2 (Figure 2e). In contrast, enforcing OTX2 activity inhibited PGCLC TF mRNA induction (Figure 2e). NANOG also directs PGCLC differentiation 20,26. Consistent with this, endogenous *Nanog* mRNA was induced precociously in $Otx2^{-/-}$ cells (Figure 2e). In addition, while *Fgf5*, *FoxD3* and *Oct6* mRNAs were not induced without OTX2 (Extended Data Figure 3f), their expression was increased above wild-type levels by OTX2 induction (Extended Data Figure 3f). These analyses suggest that OTX2 acts at the juncture between somatic and germline differentiation and inhibits PGCLC differentiation by preventing PGC TF expression.

A previous report has provided evidence for the involvement of T (Brachyury) in PGCLC induction 27 by showing that BMP4 induced T expression via endogenous wnt. We also found that T is activated robustly only when BMP4 is present (Extended Data Figure 4b) with T and other somatic markers induced during PGCLC differentiation (Extended Data Figure 4c). In vivo, BMP4 induces epiblast cells to secrete wnt28. Therefore, to assess whether wnt acts as an intermediary between BMP4 and activation of T and other somatic

markers, wnt signalling was mimicked by adding CHIR99021 to basal media (Extended Data Figure 4d). *T*, *hoxa1* and *hoxb1* mRNAs were induced by CHIR99021 but *Otx2* mRNA was repressed; effects that were reversed by addition of the wnt antagonist XAV939 (Extended data Figure 4d). Therefore, Otx2 down-regulation by BMP4 may occur via wnt signalling. To further assess this, XAV939 was added during PGCLC differentiation. XAV939 does not affect *Otx2* mRNA for 9 hours but dampens further reduction (Extended data Figure 4e). Moreover, XAV939 diminishes induction of *Blimp1* and *Prdm14* mRNAs seen after 24h (Extended data Figure 4e). This is consistent with a model in which BMP induction of wnt enforces timely repression of *Otx2* and full induction of *Blimp1* and *Prdm14*. Finally, $Otx2^{-/-}$ cells do not activate T mRNA (Extended data Figure 4c) or protein (Extended data Figure 4f). Therefore, activation of T is dispensable for PGC induction, at least when OTX2 is absent. These observations suggest that the effects of wnt signalling during PGC differentiation might be attributed to OTX2 down-regulation.

To assess whether OTX2 can interfere with the function of an established PGCLC GRN, OTX2 activity was restored at day 2, once the PGC GRN was already activated (Figure 2e). This produced a similar proportion of $SSEA1^{+}/CD61^{+}$ cells as cultures receiving no tamoxifen (Extended Data Figure 4g, h). Therefore, OTX2 does not impair the function of an established PGC network, but rather restricts the efficiency with which EpiLCs enter the germline.

PGCLC induction is considered to strictly require cytokine addition 12. Consistent with this, Oct4ΔPE::GFP was not expressed by aggregates of $Otx2^{fl/-}$ cells cultured in the absence of cytokines (Figure 3a). However, in $Otx2^{-/-}$ cells, cytokines were not essential for OctΔPE reporter activation (Figure 3a), CD61/SSEA1 surface expression (Figure 3b, Extended Data Figure 5a, b) or PGC TF expression (Extended Data Figure 5c, d). Indeed, mRNA profiling indicated that $Otx2^{+/+}$ and $Otx2^{-/-}$ EpiLCs were transcriptionally similar and that following differentiation, $Otx2^{-/-}$ cells resembled wild-type PGCLCs, irrespective of their exposure to cytokines (Extended Data Figure 6a). Principal component and ternary analysis confirmed these assessments (Figure 3c, Extended Data Figure 6b). These results indicate that without OTX2, germline entry does not require cytokines.

BLIMP1 is essential for wild-type cells to access the germline 3,4. To determine whether $Otx2^{-/-}$ cells retained this dependency, both *Blimp1* alleles were deleted from ESCs of distinct *Otx2* genotypes using CRISPR/Cas9 (Extended Data Figure1, 7a, b, c). PGCLC differentiation confirmed a BLIMP1 requirement for germline entry of OTX2-expressing cells (Figure 3d, Extended Data Figure 7d). However, deletion of *Blimp1* from $Otx2^{-/-}$ cells did not affect the ability of $Otx2^{-/-}$ cells to induce CD61/SSEA1 (Figure 3d; Extended Data Figure 7d). While deletion of *Blimp1* from wild-type cells increased expression of somatic transcripts during PGCLC differentiation, this did not occur in $Otx2^{-/-}$; $Blimp1^{-/-}$ PGCLCs (Extended Data Figure 8a). Nor did *Blimp1* removal impair the enhanced ability of $Otx2^{-/-}$ cells to activate expression of *Prdm14*, *Ap2γ*, *Nanog* or *Oct4* mRNAs (Extended Data Figure 8b) or DAZL protein (Extended Data Figure 8c). During differentiation, PGCLCs expressing OCT4 have higher H3K27me3 and lower H3K9me2 than OCT4-low cells. These relationships were maintained in $Otx2^{-/-}$ and $Otx2^{-/-}$; $Blimp1^{-/-}$ PGCLCs (Extended Data Figure 8d). Furthermore, without PGCLC cytokines, CD61/SSEA1 expression and Oct4ΔPE

reporter activation was unaffected by *Blimp1* deletion in multiple *Otx2*$^{-/-}$ cell lines (Figure 3e; Extended Data Figure 7e, f). Nevertheless, at day 6 of PGCLC differentiation, *Otx2*$^{-/-}$; *Blimp1*$^{-/-}$ cells are unable to adopt the mature PGCLC transcriptome observed in *Otx2*$^{+/+}$ or *Otx2*$^{-/-}$; *Blimp1*$^{+/+}$ cells (Figure 3c; Extended Data Figure 6). These results indicate that without OTX2, BLIMP1 is not required for phenotypic aspects of germline entry, but is required for a fully mature PGC phenotype.

While EpiLCs respond to cytokine induction by PGCLC differentiation, this ability is not maintained upon continued passaging in Activin/Fgf12, suggesting that in these conditions, cells lose germline competence. To assess whether OTX2 affects the period during which pluripotent cells remain competent for germline entry, EpiLCs were passaged in EpiLC media for a further 2 days (Figure 4a). At this point the Oct4ΔPE::GFP reporter is inactive in both *Otx2*$^{fl/-}$ and *Otx2*$^{-/-}$ cells (Extended Data Figure 9a). Cells were then transferred to PGCLC differentiation medium for 6 days. Strikingly, Oct4ΔPE::GFP was reactivated robustly in *Otx2*$^{-/-}$ but not *Otx2*$^{fl/-}$ cells (Figure 4b). Moreover, while all cell lines expressed *Blimp1* and *Ap2γ* mRNAs, CD61/SSEA1 surface expression and *Prdm14* and *Nanog* mRNA expression were observed only in *Otx2*$^{-/-}$ and not in *Otx2*$^{+/+}$ or *Otx2*$^{fl/-}$ cells (Extended Data Figure 9b, c, d). This indicates that in the absence of OTX2 the period of competence to enter the germline is extended.

To determine whether *Otx2*$^{-/-}$ cells exhibit an increased propensity to enter the germline *in vivo*, *Otx2*$^{+/+}$ or *Otx2*$^{-/-}$ ESCs constitutively expressing GFP were compared in chimaeras following morula aggregation (Figure 4c). *Otx2*$^{+/+}$and *Otx2*$^{-/-}$ cells had a comparable capacity to produce chimaeras (Extended Data Figure 9e, g). However, an enhanced proportion of *Otx2*$^{-/-}$ cells expressed BLIMP1 or SOX2 (Figure 4d; Extended Data Figure 9f), indicating that enhanced germline entry is a cell autonomous property of *Otx2*$^{-/-}$ cells.

To determine whether *Otx2*$^{-/-}$ embryos also showed enhanced PGC numbers, *Otx2*$^{+/-}$ mice15 were intercrossed and *Otx2*$^{-/-}$ embryos analysed at E7.5. These embryos show strong developmental defects15,16 but also showed increased PGC numbers (Figure 4e, Extended Data Figure 10 a, b), confirming that in vivo, OTX2 acts as a negative regulator of the PGC programme.

Previous studies have shown that, in the mouse, competence to enter the germline exists transiently in embryos from E5.5-6.25 1. In wild-type cells, germline entry requires BMP4 signalling from the extraembryonic ectoderm 2 and is critically dependent on the downstream action of BLIMP1 3. Our work identifies OTX2 as an intermediary fulcrum in these processes (Figure 4f). During the period of PGC competence BMP4 represses *Otx2* expression, partly by endogenous wnt activation (Figure 4g). This reduction in OTX2 is necessary for expression of the PGC TFs BLIMP1, PRDM14, AP2γ and NANOG since enforcing OTX2 activity prevents their expression. Moreover, the rate of Otx2 decline appears important since without cytokines, germline entry is diminished. We propose that without cytokines, the window for germline entry closes before OTX2 is reduced below a threshold necessary for PGC TF expression. Furthermore, in the absence of OTX2, PGC TF expression does not require BMP4, indicating that BMP4 functions by repressing *Otx2*. *Otx2*$^{-/-}$ cells also exhibit an extended competence period, suggesting that OTX2 sets in train

a mechanism that defines the extent of the competence period. Also, as *Otx2*$^{-/-}$ cells can initiate PGC differentiation without BLIMP1, this suggests a reciprocal relationship between BLIMP1 and OTX2, in which BLIMP1 represses 21,29,30 and OTX2 activates somatic gene expression 17. Supporting this, during PGCLC differentiation *Otx2*$^{-/-}$ cells do not activate mesendoderm genes17 (Extended Data Figure 4c) that are otherwise repressed by Blimp1 30. This may explain why some aspects of PGCLC differentiation phenotype can be divorced from a Blimp1 requirement in *Otx2*$^{-/-}$ cells. This places OTX2 at a developmental crossroads where it acts to police excessive access to the germline (Figure 4f).

Finally, our findings are noteworthy in light of the hypothesis that the neural lineage is the default developmental pathway for vertebrate cells31. Interestingly, neural induction requires inhibition of BMP signalling 32. BMP is a known facilitator of germline entry2 and is identified here as a key *Otx2* repressor. The default neural induction hypothesis is based principally on studies in chicks and frogs, species in which PGCs are formed by germplasm segregation. Yet, induced germline segregation is considered the ancestral mechanisms that predates the recurrent evolution of germplasm 7,8. The highly efficient entry of pluripotent cells into the germline in the absence of OTX2 reported here suggests that the germline may be the ancient default option that must be overcome in order to elaborate the ancillary structures of the soma.

Methods

All mouse studies were performed in accordance with UK Home Office regulations under project licence PPL 60/4435 and carried out in a Home Office-designated facility.

Cell culture and differentiation

ESCs were routinely cultured in GMEMβ supplemented with 100U/ml LIF and 10% FCS at 3-10 x 10^5 cells/cm^2 density on tissue culture flasks coated with 0.1% gelatin33. EpiLC differentiation and PGCLC induction were carried out according to protocol previously described 12,34,35.

For cytokine-free differentiation, EpiLCs were dissociated and resuspended at 8 x 10^4 cells/ml in GK15 medium (GMEMβ supplemented with 15% KOSR). 25μl drops containing 2,000 cells were plated on the lids of tissue culture dishes and incubated over a reservoir of PBS for 2 days. Hanging drops were then collected and transferred to untreated culture dishes supplemented with GK15 medium and rotated at 72 rpm. Fresh medium was replenished every other day. CHIR (3μM) and XAV939 (2μM) were used to induce and repress wnt signalling.

Generation of knockout cell lines

For a summary of cell lines used in this report and a history of their derivation, see Extended Data Figure 1.

Otx2 knockout (*Otx2*$^{lacZ/GFP}$) and Otx2 conditional knockout (*Otx2*$^{lacZ/fl}$; *Rosa26*$^{CreER/+}$) cell lines and targeting strategies have been described previously18. To derive Otx2KO (*Otx2*$^{lacZ/-}$) lines from Otx2$^{lacZ/fl}$, Otx2$^{lacZ/fl}$, ESCs were treated with 1μM tamoxifen for 24

hours, plated at clonal density and after 6 days, individual colonies picked, expanded and genotypes verified with qPCR, western blot and immunostaining.

For KO cell lines derived using Crispr/Cas9 technology, ESCs were transfected with vectors expressing gRNAs and eSpCas9-T2A-mCherry or eSpCas9-T2A-eGFP using Lipofectamine 3000 (Invitrogen, L3000015) and cultured for 24 hours. After FACS sorting, single cell clones were expanded and genotyped. Clones with predicted genotypes were further verified with qPCR or western blot and immunostaining. See Supplementary Table 1 for detailed oligonucleotide sequences of gRNAs, genotyping PCR.

Immunohistochemistry

For whole-mount staining of embryos and PGCLC aggregates, embryos and PGCLC aggregates were fixed with 4% paraformaldehyde (PFA) in PBS (RT, 30min). For Fragilis staining, embryos were washed three times in PBS/0.1%BSA and blocked overnight at 4°C in 3% donkey serum (Sigma)/1% BSA/PBS solution. For other antibodies, samples were washed three times with PBS/0.1% TritonX100 (PBST), permeabilized in 0.5% Triton X100/PBS solution for 15 minutes and incubated in 1 M glycine in PBST for 20 minutes. After three washes, samples were blocked overnight at 4°C using 3% donkey serum, 1% BSA (Sigma) in PBST (blocking buffer). Samples were then incubated for 72 hours with diluted primary antibodies, rinsed four times for 20 min each in PBST and incubated for 4 hours at RT with diluted secondary antibody. Samples were then rinsed four times for 20 min each in PBST. DAPI (Molecular Probes, D1306) was used for nuclear staining (same for other staining). For imaging, embryos were treated with 10%, 25%, 50%, 97% thiodiethanol (Sigma, 166782) for 5min in each gradient and were imaged using the TCS SP8 inverted confocal microscope (Leica).

For frozen sections staining, aggregations were fixed in 4% PFA (RT, 20 min). After washing in PBS, samples were embedded in Tissue-Freezing medium (Thermo Fisher scientific, 6502Y) and sectioned at a thickness of 5μm. For antigen retrieval, sections were microwaved with highest power in 10mM sodium citrate (PH=6.0) for 2 min 30s, twice. After antigen retrieval, samples were incubated in blocking buffer (RT, 1 hour), then incubated with primary antibodies (4 °C overnight), after rinsed three times in PBST for 10 min, incubated for 2 hours at RT with diluted secondary antibody. Sections were then covered by cover slip in Fluoromount (SouthernBiotech, 0100-01) and imaged using the TCS SP8 inverted confocal microscope (Leica)

For immunostaining of cells grown in monolayer, cells were washed once with PBS, fixed in 4% PFA (RT, 10 min), permeabilised in 0.3% Triton X100/PBS (RT, 20 min), incubated in blocking buffer (RT, 1 hour), before addition of primary antibodies and incubation at 4°C overnight. Cells were washed in PBST (4 times, 5 mins) before incubation with diluted secondary antibodies (RT, 1 hour). After washing 4 times (PBST), cells were imaged using the TCS SP8 inverted confocal microscope (Leica).

For cytospin staining, cells or aggregates were dissociated into single cells. 1 $\times 10^5$ cells in 100μl 1%BSA/PBS buffer were added into sample holders, centrifuged in the cytospin machine (5 min, 1200rpm). Microscope slides were then taken from the holders and cells

circled with hydrophobic marker pen. Staining was then finished following the same protocol as for monolayer cells.

For PGC cell counting in wild-type and *Otx2*-null embryos, embryos were isolated at embryonic day (E) 7.5, washed in PBS, fixed overnight in 4% PFA/PBS, dehydrated and paraffin embedded as reported18. Embryos were sectioned in coronal-frontal or sagittal sections and processed for immunohistochemistry (IHC) with antibodies against Blimp1, AP2γ (Santa Cruz Biotechnology, SC-53162) and Fragilis (R&D Systems, AF3377). All sections were analyzed and those including PGCs captured for cell-counting analysis.

If not specified, primary and secondary antibodies used are listed in Supplementary Table 2.

Immunofluorescence quantification

Cytospin slides were stained at the same time and imaged using a Zeiss Observer microscope (Zeiss), Plan-Apo 20x NA, 0.8 objective (Zeiss), a Hamamatsu ORCA-Flash4.0 V3 camera (Hamamatsu), a Colibri 7 (Zeiss) light source and the following filter cubes (name, excitation LED, beam splitter, band pass emission filter, 49 DAPI - 395 - 480/40; 38 HE GFP - 495 - 525/50; 43 HE dsRed - 570 - 605/70; Cy5-660-700/775). Images were analysed using CellProfiler software (version 2.2.0)36. DAPI staining was first used to segment individual nuclei based on the diameter and intensity of the objects (25-90pixel units and intensity threshold > 0.05 respectively), then the intensity of Otx2 and Ap2γ of the segmented nuclei were measured and the mean intensity of each channel reported. Over 8000 segmented nuclei of each samples were analyzed. The data were analysed in R and plot were generated using the ggplot2 package. The Otx2 KO EpiLCs are negative for both Otx2 and Ap2γ staining and therefore were used to set up the threshold for gating Otx2 and Ap2γ for all samples (negative gate >99.5%).

Flow cytometry

FACS analysis was performed as described34. Cells grown in monolayer or embryoid bodies in suspension were dissociated into single cells with trypsin and neutralised in PBS/10%FCS. A maximum of $5x10^5$ cells were collected by centrifugation and the pellet resuspended in 100µl PBS/10%FCS supplemented with Alexa Fluor® 647 anti-mouse/human CD15 (SSEA-1) (Biolegend, 125608) and PE anti-mouse/rat CD61 (Biolegend, 104307) diluted 1/200 and 1/500 respectively and incubated (30 mins, 4°C). Cells were washed twice in 1 ml PBS/10% FCS before analysis on a BD Fortessa 5 laser LSRII. Gate strategy was shown in Extended Data Figure 3a.

SDS-PAGE Electrophoresis and Immunoblotting

Immunoblot analysis was performed as described37. Briefly, Protein samples from cell lysates, along with protein ladder (Novex, cat. LC5925) were loaded on 10% Bis-Tris Gels (Novex, cat. BG00102BOX) and electrophoresis performed at 200V for 60-80 minutes. Proteins were then transferred onto Nitrocellulose membrane (Capitol Scientific, cat. 10401396), blocked in 10% milk (w/v) (RT, 1 hour), followed by incubation with primary antibodies (4°C, overnight). After 3 washes in PBST membranes were incubated with IRDye conjugated secondary antibody, followed by 3 washes in PBST before being visualised in

Europe PMC Funders Author Manuscripts

LI-COR Odyssey Imaging Systems. Primary and secondary antibodies were listed in Supplementary Table 2.

RNA analysis

Total RNA was extracted using either Trizol (Invitrogen,15596026) or RNeasy micro (Qiagen, 74034) or mini kit (Qiagen, 74104) following the manufacturer's instructions, followed by DNase treatment (Qiagen, 157047207). Reverse transcription reactions were performed using Superscript First Strand Synthesis kit (Invitrogen, 1964419) and quantitative PCR performed using SYBR® Green Kits (Takyon, UF-NSMT-B0701) on Roche LightCycler 480 with cDNA equivalent of 25ng total RNA per reaction. Values for each gene were normalised to expression of TATA-box Binding Protein (TBP) according to 2−ΔCT formula38. Oligonucleotide sequences are shown in Supplementary Table 3.

Transcriptomic Profiling and Data analysis

Total RNAs were extracted using RNeasy Plus Micro Kit (Qiagen, Cat.74034), following supplier's instructions. RNAs were labelled using Illumina® TotalPrep™ RNA Amplification Kit (Illumina, Cat.AMIL1791) following manufacturer's instructions. Briefly, 100~300ng total RNA were reverse transcribed using oligodT primers, followed by 2nd strand cDNA synthesis. The dsDNAs were then in vitro transcribed into biotin labelled complementary RNA (cRNA) at 37°C for 12 hours. The cRNAs were purified and quality analysed using Agilent Bioanalyzer 2100. The hybridizations were performed by the Eurofins Genomics AROS in Denmark. The samples were hybridized on Illumina MouseWG-6 v2 BeadChip. A signal intensity (expression) value and a detection p-value (whether the signal is above background) for each probe on the array was obtained using Illumina GenomeStudio software with standard settings. A total of 13,683 probes which had detection p-value <0.01 in at least three experiments were considered for further analysis. A variance-based filtering of gene expressions was performed using the genefilter package with variance cutoff of 0.75, leaving 3,421 probes for further statistical analysis. Unsupervised hierarchy clustering, generation of heatmap and PCA and ternary plot were carried out by means of R (https://www.R-project.org) using the following packages: cluster, pheatmap, FactoMineR, ggtern and RColorBrewer. The microarray data has been deposited in the GEO database under accession number GSE116640.

Embryo aggregation

E2.5 embryos were collected from superovulated F1 (CBA male cross with C57BL/6J female) females with M2 buffer (Sigma, M1767). After cultured in KSOM (Millipore, MR-020P-5F) for 15min, zona pellucidae were removed by Tyrode's solution (Sigma, T1788) and embryos cultured in KSOM in aggregation plates prepared by aggregation needle (BLS, DN-10). Wildtype E14Tg2a ESCs and two independent *Otx2* knockout cell lines (labelled with Flag-GFP) were used for aggregation. Cells were trypsinized (37 °C, 1min), washed and resuspended with GMEM/FCS medium. Each embryo was aggregated with 6-8 cell clumps and cultured in the incubator. The next day, good quality blastocyst were picked and transferred to E0.5 CD1 recipient 39.

Extended Data

Europe PMC Funders Author Manuscripts

Europe PMC Funders Author Manuscripts

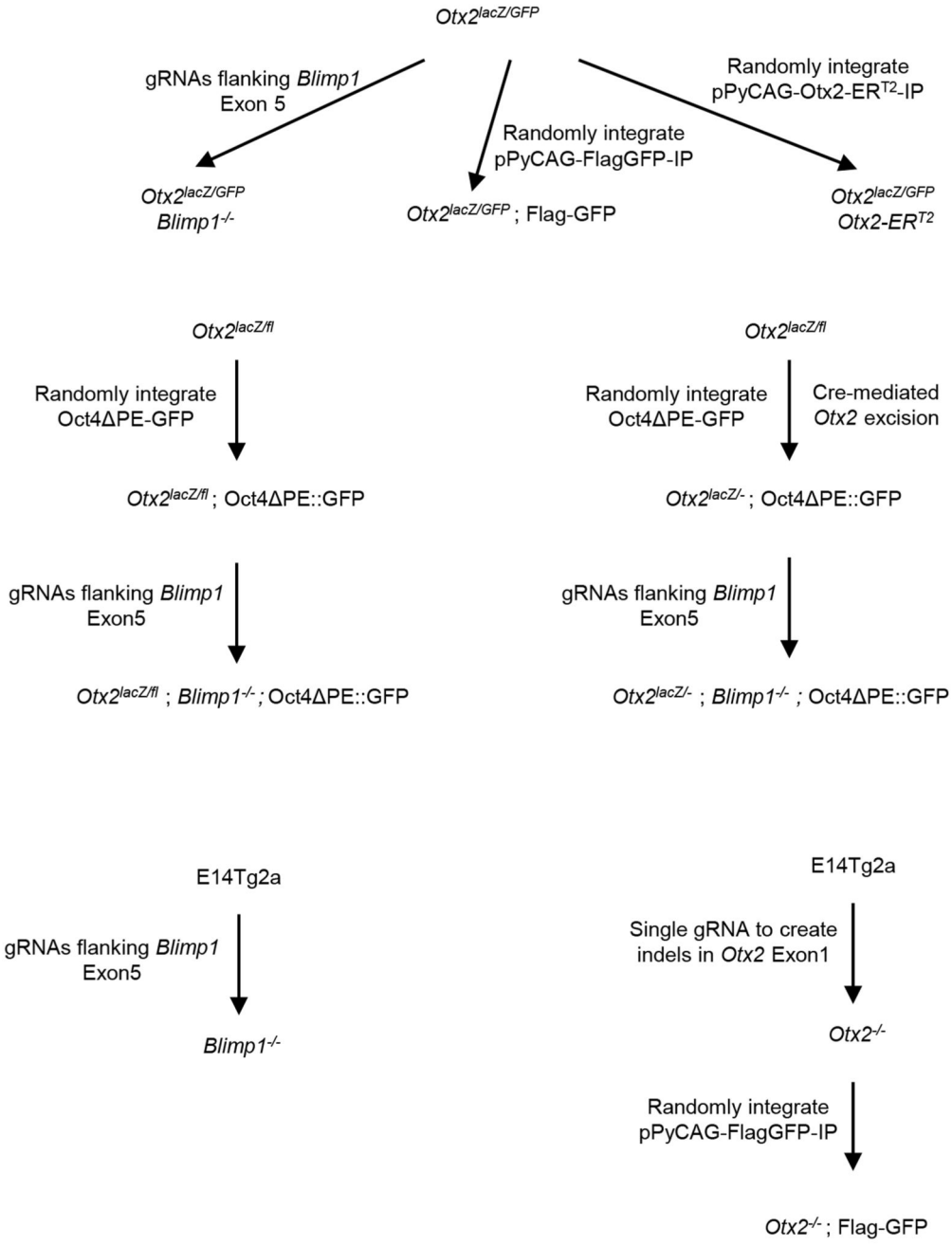

Extended Data Figure 1. Summary of cell lines used in this report.

Otx2$^{lacZ/GFP}$ and *Otx2*$^{lacZ/fl}$ ESCs have been described previously. Summarized below are further modifications to *Otx2* or *Blimp1*, or transgene additions in the above or wild-type backgrounds. Further schematic details illustrating the points of Cas9 modification of *Otx2* or *Blimp1* and genotype verification of derived cell lines are shown in Extended Data Figure 3 or 6, respectively.

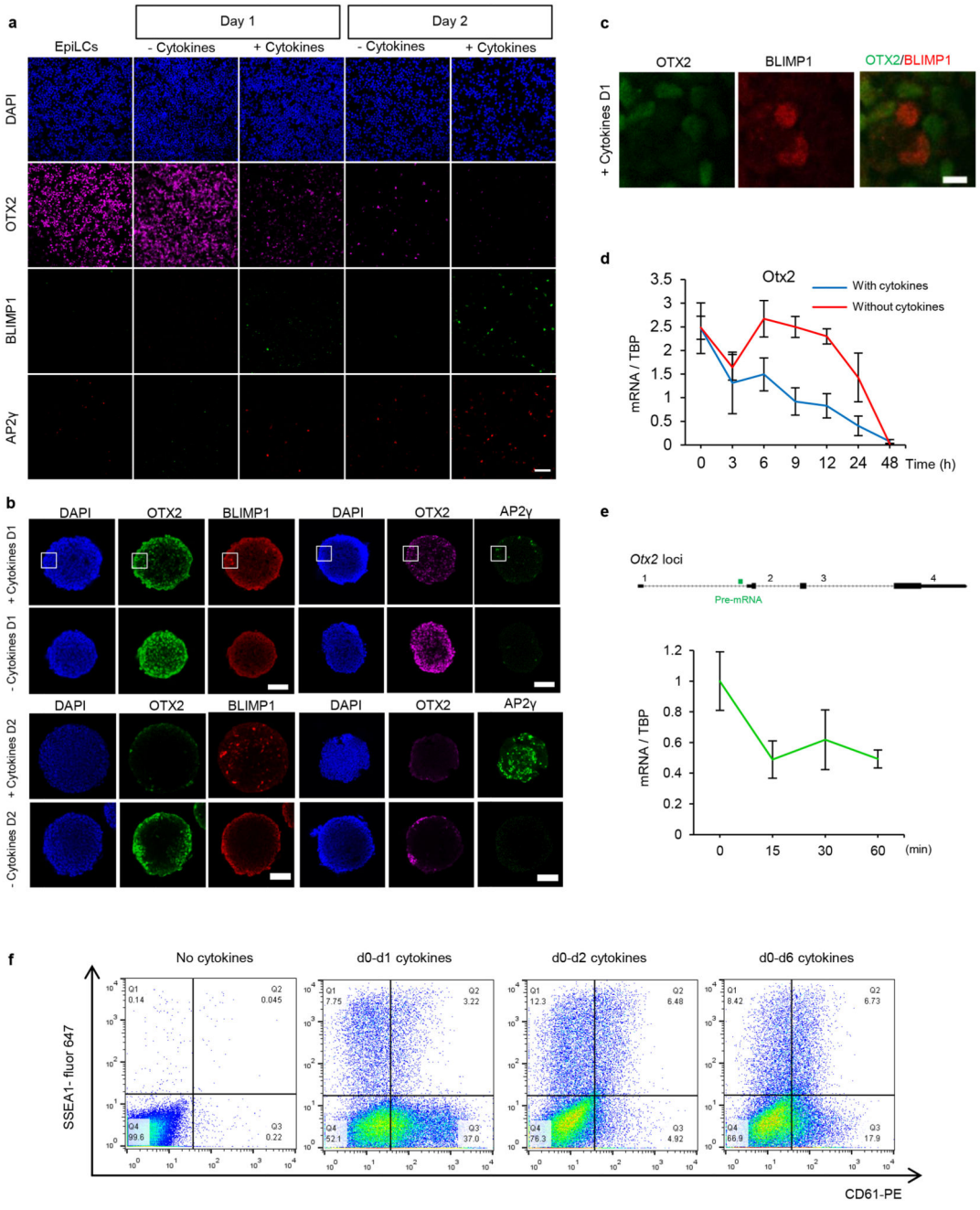

Extended Data Figure 2. Competence for germline entry is preceded by downregulation of OTX2 protein.

a. Representative cytospin images of OTX2, BLIMP1 and AP2γ staining using E14Tg2a aggregates after 1 day or 2 days of PGCLC differentiation. n=2. Scale bar; 100 μm.

b. Whole mount immunofluorescence of E14Tg2a aggregates after 1 (D1) or 2 days (D2) of differentiation of EpiLCs in the presence or absence of cytokines. Representative images of OTX2 and BLIMP1 are shown. n=3. Scale bar; 50 μm.

c. Magnified image of the region highlighted in b. Scale bar; 10 μm.

d. Quantitative transcript analysis of Otx2 in E14Tg2a cultures with (n=4) or without cytokines (n=7) at indicated time point (h, hours). Schematic illustration is shown in Figure 1b. Expression levels are normalised to TBP; Values are means±SD.
e. Top, primers used for Otx2 pre-mRNA transcript analysis are shown relative to the primary transcript structure. Bottom, quantitative transcript analysis of Otx2 pre-mRNA at the indicated times (minutes) after changing E14Tg2a EpiLCs into PGCLC medium. Expression levels are normalised to TBP and shown relative to expression at t = 0; Values are means±SD, n= 3 biologically independent replicates. **f.** Assessing the temporal requirement of cytokine treatment for efficient PGCLC induction. Aggregates of E14Tg2a EpiLCs treated with cytokines for 1 (d0-d1), 2 (d0-d2) or 6 days (d0-6) were assessed by flow cytometry for surface expression of SSEA1 and CD61 at day 6 of PGCLCs differentiation. n=3.

Europe PMC Funders Author Manuscripts

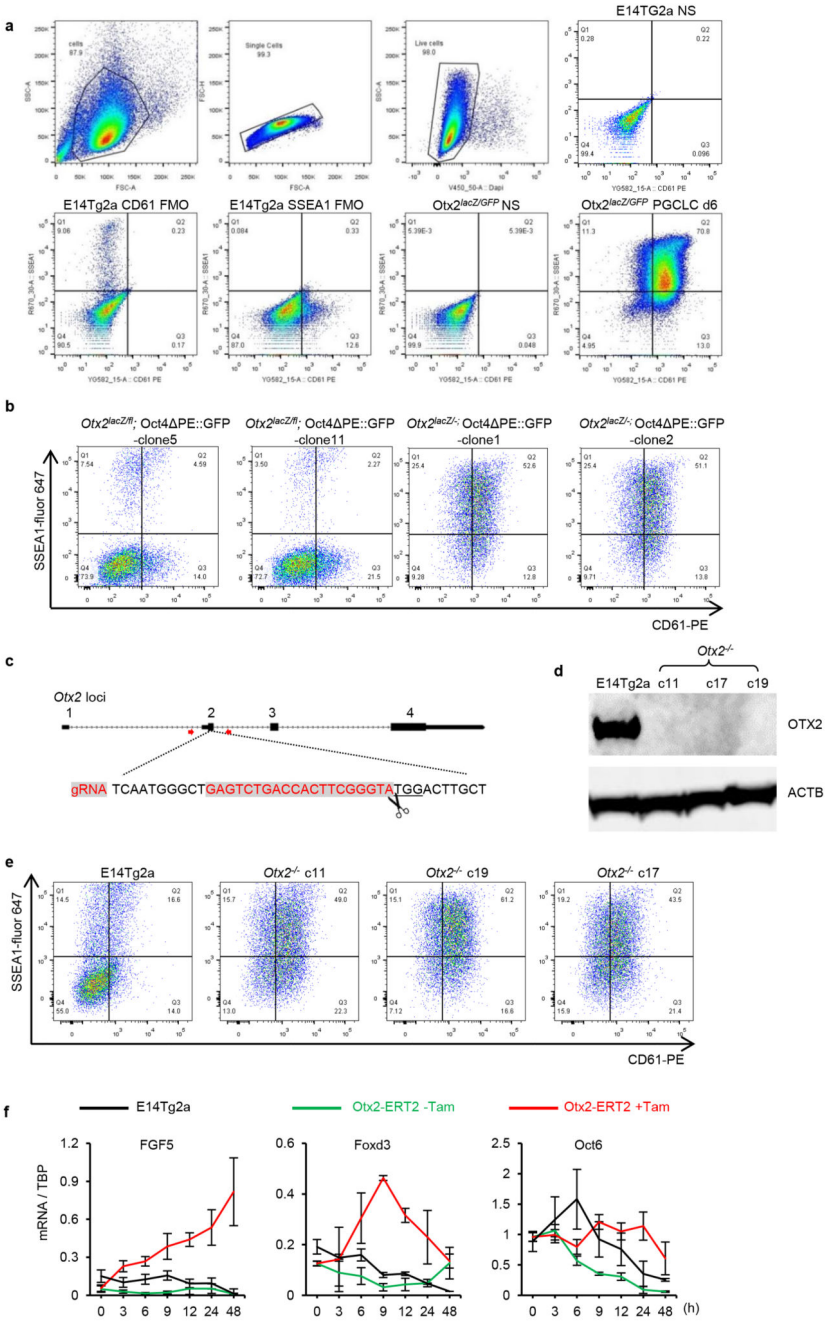

Extended Data Figure 3. Independent *Otx2*$^{-/-}$ clones show enhanced PGCLC induction efficiency.

a. The gating strategies for analysing PGCLCs by flow cytometry. Cells were first gated based on the FSC (size) and SSC (complexities) scatter plot, followed by selection for singlets based on linear correlations between FSC-area and FSC-height. Live cells were then gated based on exclusion of DAPI to indicate cell membrane integrity. Live cells were then analysed for SSEA1 and CD61. Cells stained for fluorescence minus one (FMO) were used to set gates; stained and non-stained cells are also shown.

Europe PMC Funders Author Manuscripts

b. *Otx2*$^{lacZ/fl}$ and *Otx2*$^{lacZ/-}$ cells with the Oct4ΔPE::GFP reporter (2 independent clones each) were assessed by flow cytometry for surface expression of SSEA1 and CD61 at day6 of PGCLC differentiation. For clone 5 and clone 1, n=2; for clone 11and clone 2, n=9

c. Diagram showing the gRNA sequence (in red) and targeting strategy for generating *Otx2* knockout cell lines. Red arrows represent genotyping primers used for screening clones.

d. Immunoblot analysis of OTX2 protein expression in EpiLCs of E14Tg2a and three *Otx2*$^{-/-}$ clones. Experiment preformed once.

e. E14Tg2a and 3 independent *Otx2*$^{-/-}$ clones generated by CRISPR/Cas9 were assessed by flow cytometry for surface expression of SSEA1 and CD61 at day 6 of PGCLC differentiation. 2 biologically independent experiments for clone c11, one for clone c17 and c19.

f. Q-RT-PCR of epiblast markers during the time-course outlined in Fig 1b. Expression levels are normalised to TBP; h, hours; Values are means±SD, n= 3 biologically independent replicates.

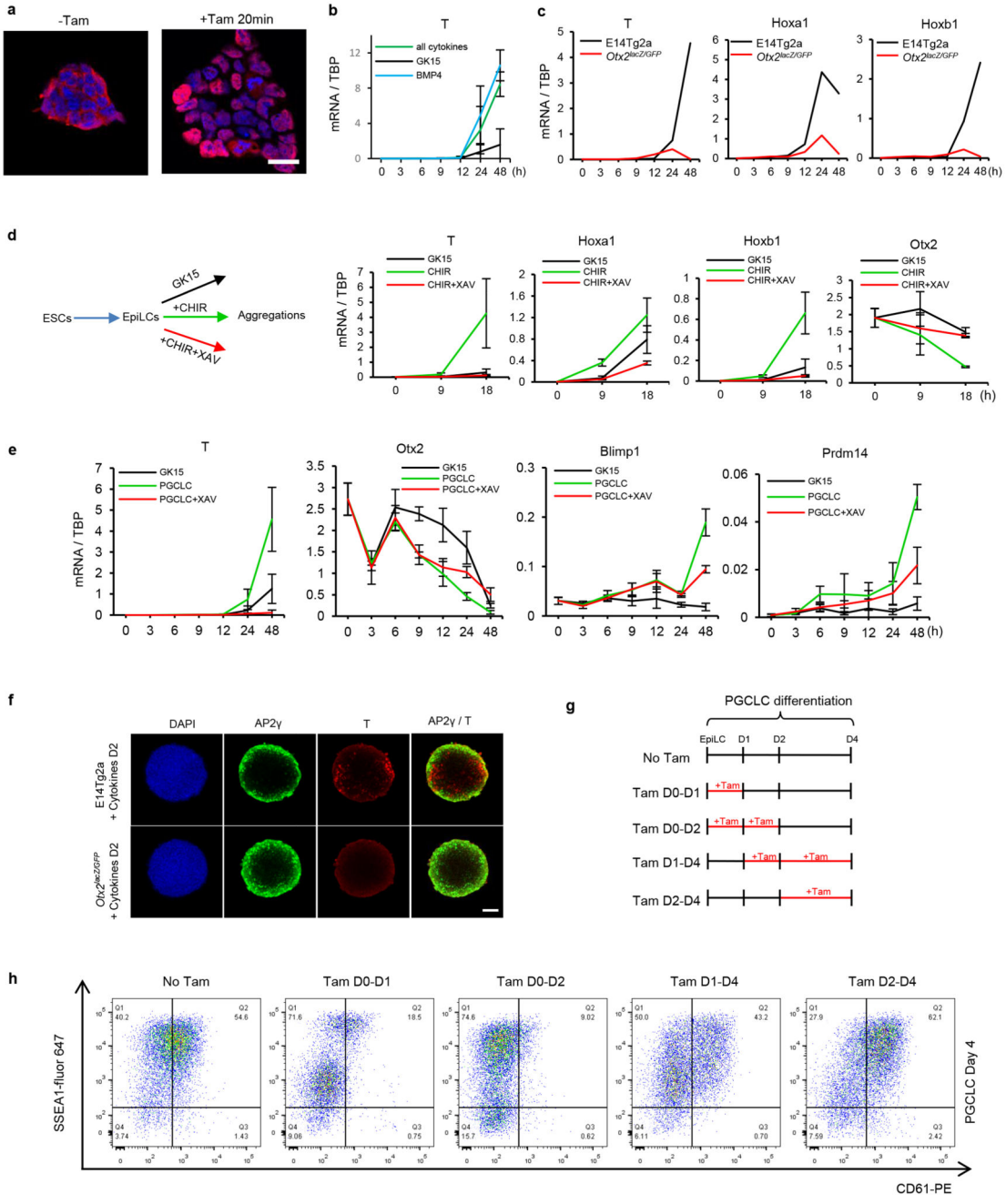

Extended Data Figure 4. OTX2 restricts PGC specification during the first 2 days of induction.

a. OTX2 immunofluorescence of *Otx2*$^{lacZ/GFP}$::Otx2ER^{T2} ESCs before or after treatment with tamoxifen for 20min, n= 2 biologically independent experiments. Scale bar=20um.

b. Quantitative transcript analysis of T (Brachyury) during the time-course outlined in Figure 1b in basal GK15 medium supplemented with the indicated cytokines. Expression levels are normalised to TBP; Values are means±SD, n= 3 biologically independent replicates.

Europe PMC Funders Author Manuscripts

c. Quantitative transcript analysis of T (Brachyury), Hoxa1 and Hoxb1 during the time-course outlined in Figure 1b in indicated cell lines. Expression levels are normalised to TBP; values are means from 2 biologically independent replicates.

d. Left: scheme illustrating the strategy for induction or repression of wnt signalling. E14Tg2a EpiLCs were aggregated in the indicated media and transcripts analysed at 0, 9 and 18 hours. Right: Quantitative transcript analysis of T (Brachyury), Hoxa1, Hoxb1 and Otx2 during the time-courses outlined on the left. (h, hours). Expression levels are normalised to TBP; Values are means±SD, n= 3 biologically independent replicates.

e. Quantitative transcript analysis of T (Brachyury) Otx2, Blimp1 and Prdm14 during E14Tg2a differentiation in three different media conditions (GK15, without cytokines; PGCLC, GK15 with cytokines; PGCLC +XAV, GK15 with cytokines and with XAV939) at the indicated time point (h, hours). Expression levels are normalised to TBP; Values are means±SD, n= 3 biologically independent replicates. **f.** Whole mount immunofluorescence analysis of AP2γ and T (Brachyury) in E14Tg2a and $Otx2^{lacZ/GFP}$ day2 (D2) PGCLC aggregates. n=2 biological replicates. Scale bar; 50 μm.

g. Scheme illustrating tamoxifen administration schemes.

h. *Otx2*$^{lacZ/GFP}$::$Otx2ER^{T2}$ cells were assessed by flow cytometry for surface expression of SSEA1 and CD61 at days 6 of PGCLC differentiation following the tamoxifen treatment regime outlined (**b**). n=2 biological replicates.

Europe PMC Funders Author Manuscripts

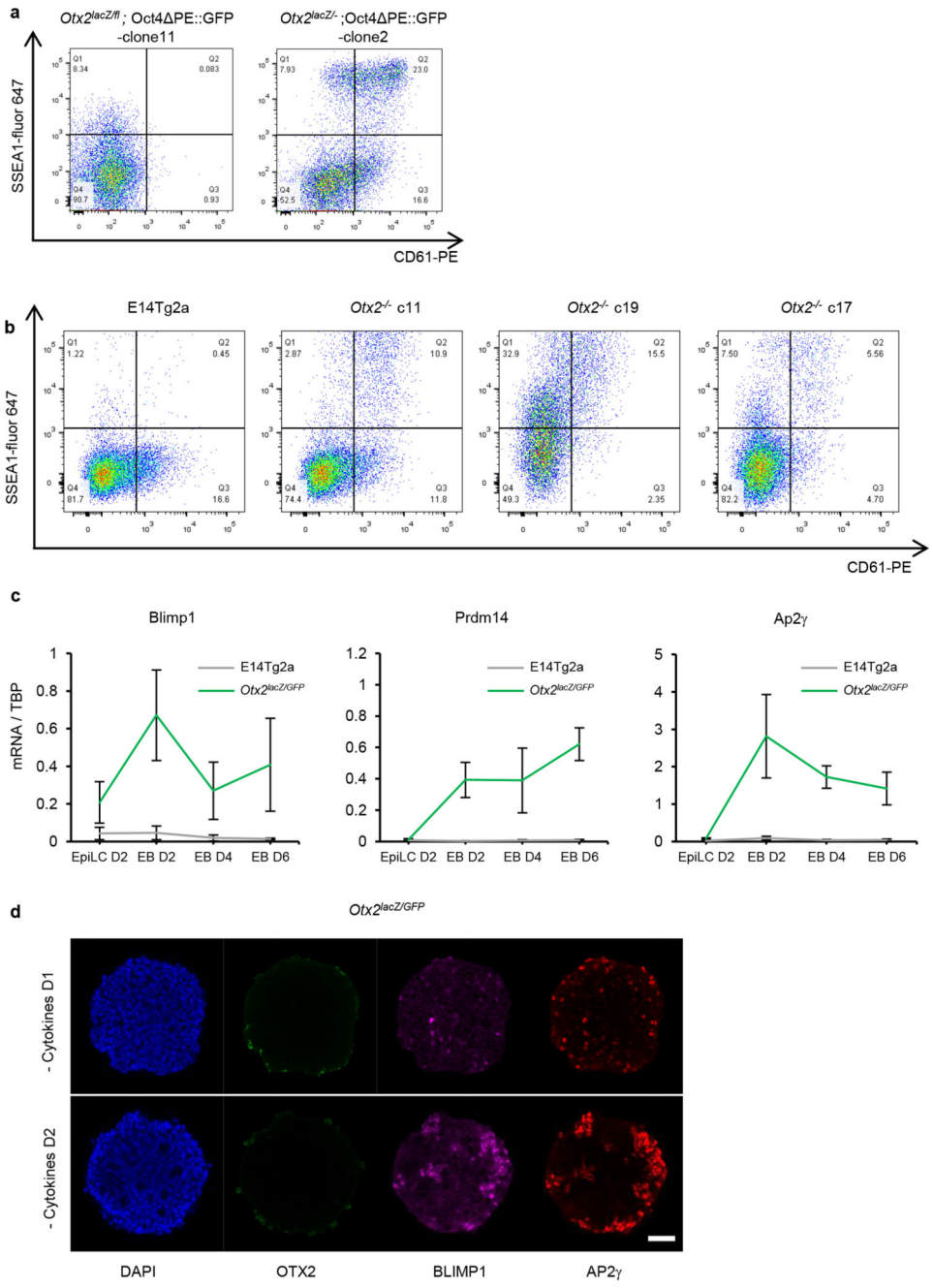

Extended Data Figure 5. PGCLC differentiation of *Otx2*–null cells in the absence of cytokines.

a. *Otx2*$^{lacZ/fl}$ and *Otx2*$^{lacZ/-}$ cells carrying the Oct4ΔPE::GFP reporter (aggregates shown in Figure 3a) were assessed by flow cytometry for surface expression of SSEA1 and CD61 at day 6 of PGCLC differentiation in the absence of cytokines. n=7.

b. E14Tg2a and 3 independent *Otx2*$^{-/-}$ clones generated by CRISPR/Cas9 were assessed by flow cytometry for surface expression of SSEA1 and CD61 at day 6 of PGCLC differentiation in the absence of cytokines. 2 biologically independent experiments for clone c11, one for clone c17 and c19.

c. Quantitative transcript analysis of mRNAs encoding PGC TFs during differentiation without PGCLC cytokines at indicated time point. Expression levels are normalised to TBP; Values are means±SD, n= 3 biologically independent replicates.

d. Wholemount immunostaining of aggregates of *Otx2*$^{lacZ/GFP}$ cells at day 2 in the absence of cytokines for OTX2, BLIMP1 and AP2γ. Bar; 40μm. n=3.

Europe PMC Funders Author Manuscripts

Europe PMC Funders Author Manuscripts

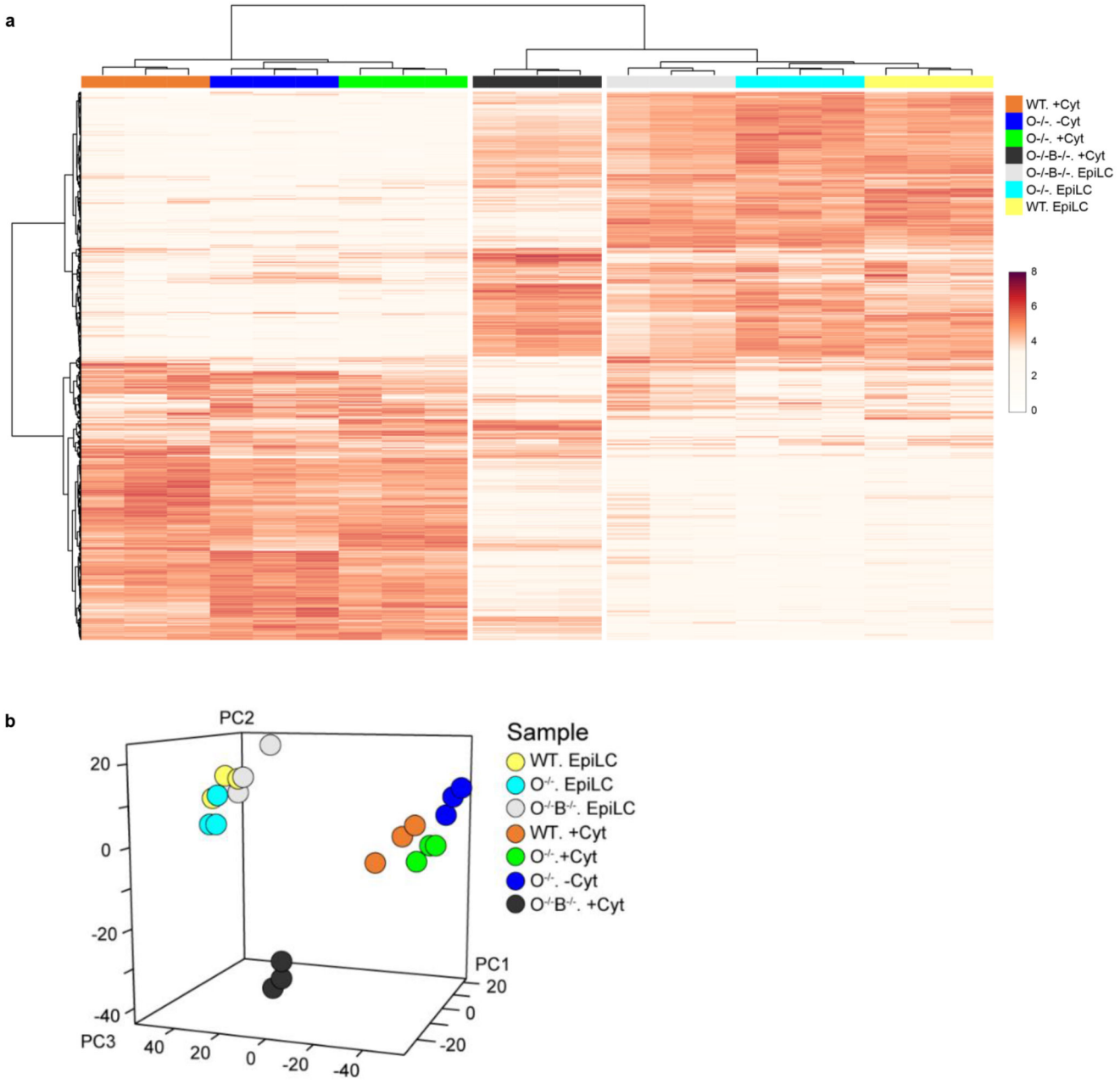

Extended Data Figure 6. Transcriptome analysis of EpiLCs and day6 PGCLCs.

a-b. Heatmap of the normalized gene expression and and principal component analysis of microarray data (from 3 biologically independent replicates under 7 different conditions) ordered by unsupervised hierarchical clustering; rows correspond to transcripts and columns to cells. Differentiations performed in the presence (+Cyt) or absence (-Cyt) of cytokines are indicated. WT, E14Tg2a; $O^{-/-}$, *Otx2*$^{lacZ/GFP}$; $O^{-/-}$ $B^{-/-}$, *Otx2*$^{lacZ/GFP}$; *Blimp1*$^{-/-}$.

Europe PMC Funders Author Manuscripts

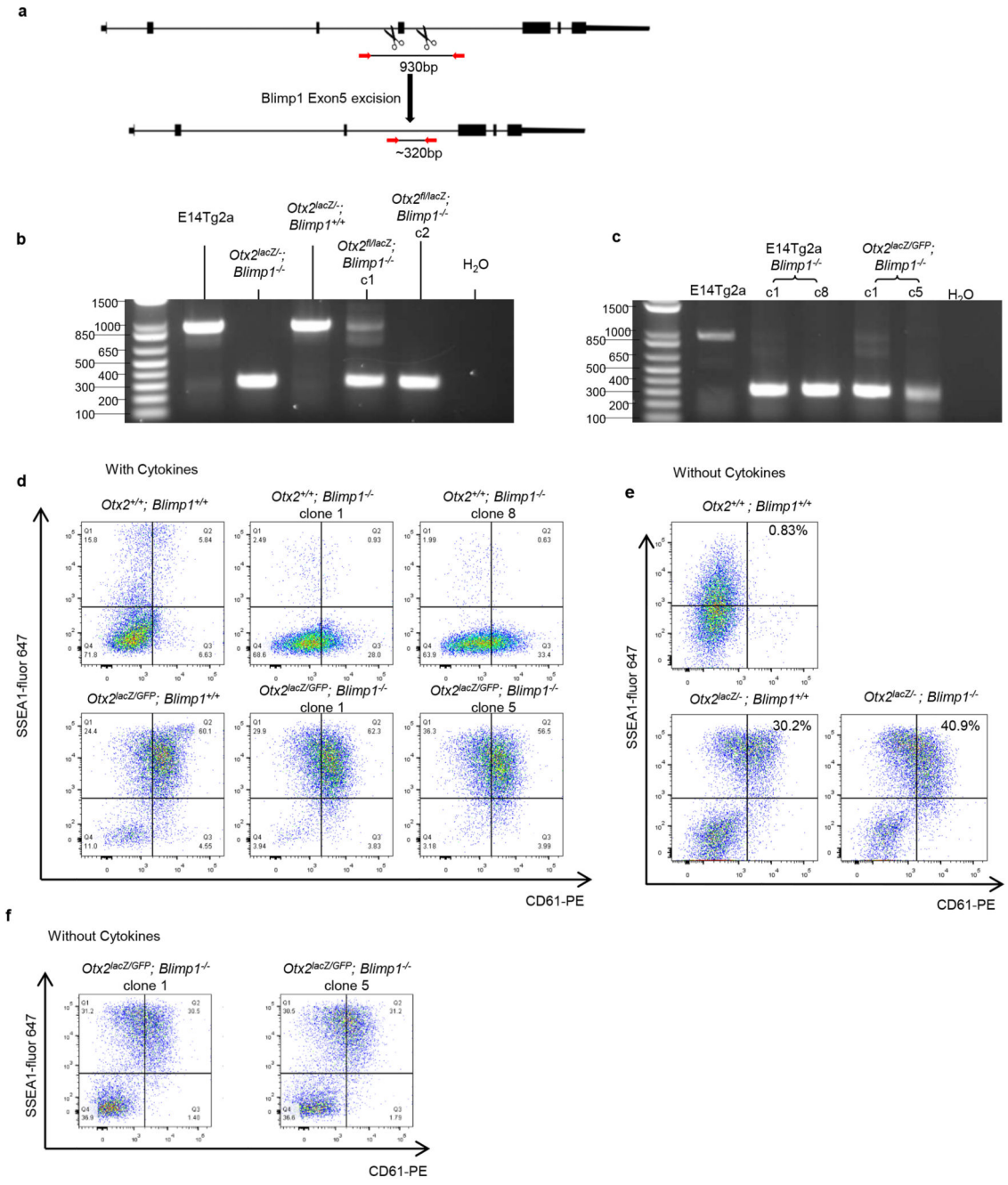

Extended Data Figure 7. PGCLC induction of independent *Blimp1*-null cell lines.

a. Scheme showing the strategy used to generate *Blimp1* KO cell lines. A pair of gRNAs flanking *Blimp1* exon5 were co-expressed to ensure complete deletion of *Blimp1* exon5. Red arrows represent genotyping primer pairs used to screen clones.

b, c. *Blimp1*-null clones used in Figure 3 (b) or Extended Figure 8d (c) were genotyped using primers indicated in **a**. n= 2 biologically independent replicates for both, all clones have been sequenced.

d. Cells of the indicated genotypes (**c**) were assessed by flow cytometry for surface expression of SSEA1 and CD61 at day 6 of aggregation in the presence of PGC induction cytokines. n=2

e-f. Cells of the indicated genotypes (**c**) were assessed by flow cytometry for surface expression of SSEA1 and CD61 at day 6 of aggregation in the absence of PGC induction cytokines. n=2

Europe PMC Funders Author Manuscripts

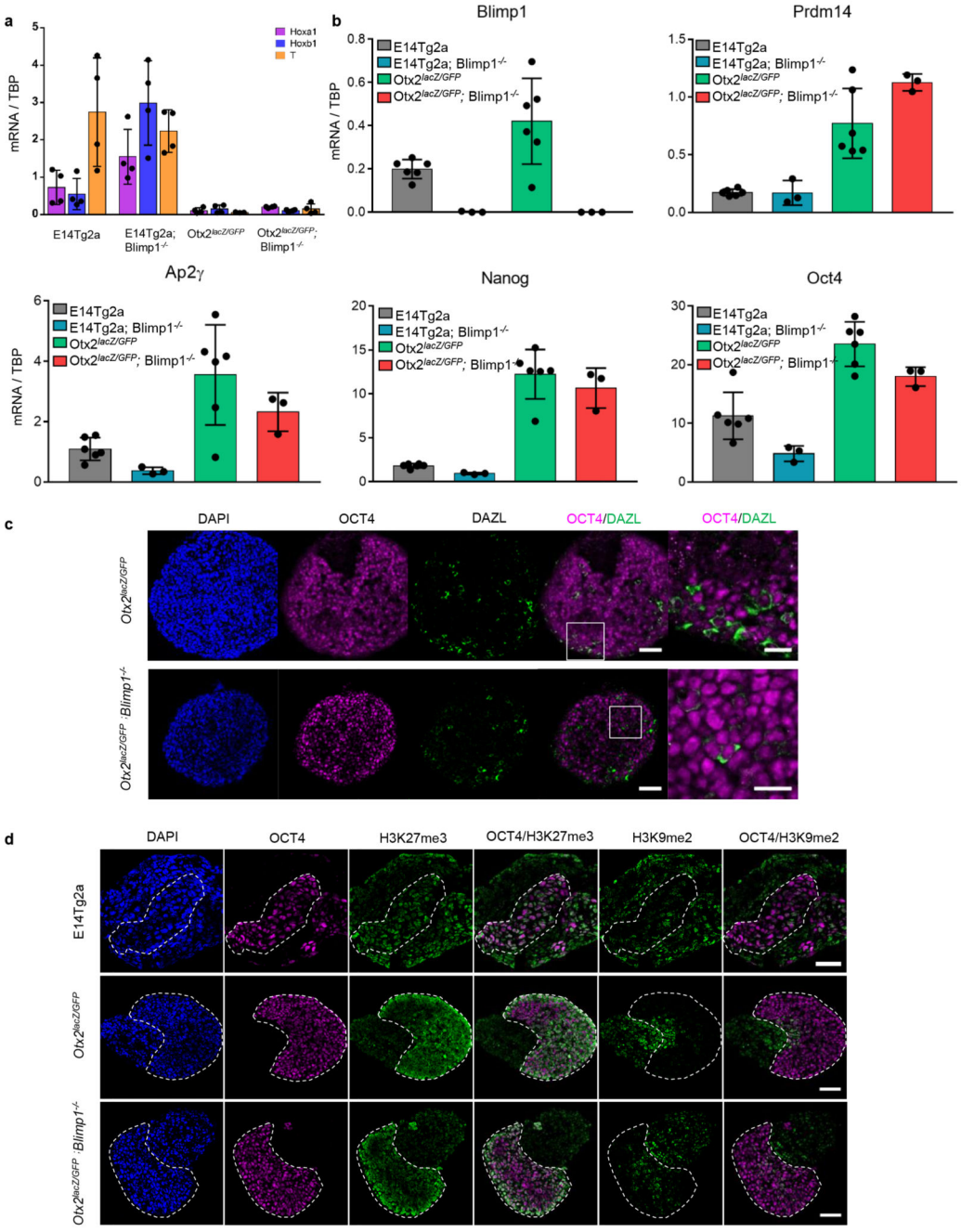

Extended Data Figure 8. *Otx2*$^{-/-}$; *Blimp1*$^{-/-}$ PGCLCs activate PGC markers.

a. Quantitative analysis of somatic transcripts at day 2 of PGCLC induction in the indicated cell lines. Expression levels are normalised to TBP; Values are means ± SD; n=4 biological replicates, each dot represents the value from one experiment.

b. Quantitative analysis of PGC TF transcripts at day 2 of PGCLC induction in the indicated cell lines. Expression levels are normalised to TBP; Values are means ± SD; n=6 biological replicates for E14Tg2A and *Otx2*$^{lazZ/GFP}$, and 4 for Blimp1 KO cell lines each dot represents the value from one experiment.

Europe PMC Funders Author Manuscripts

c. Immunofluorescence staining for OCT4 and DAZL of cryo-sections of *Otx2*$^{lacZ/GFP}$ and *Otx2*$^{lacZ/GFP}$; *Blimp1*$^{-/-}$ aggregates at day6 of PGCLC induction. Bar; 50μm and 20μm. n= 2 biologically independent replicates.

d. OCT4, H3K27me3 and H3K9me2 immunofluorescence analysis of cryo-sections of E14Tg2a, *Otx2*$^{lacZ/GFP}$ and *Otx2*$^{lacZ/GFP}$; *Blimp1*$^{-/-}$ aggregates at day6 of PGCLC induction. Bar; 50μm. n= 2 biologically independent replicates.

Europe PMC Funders Author Manuscripts

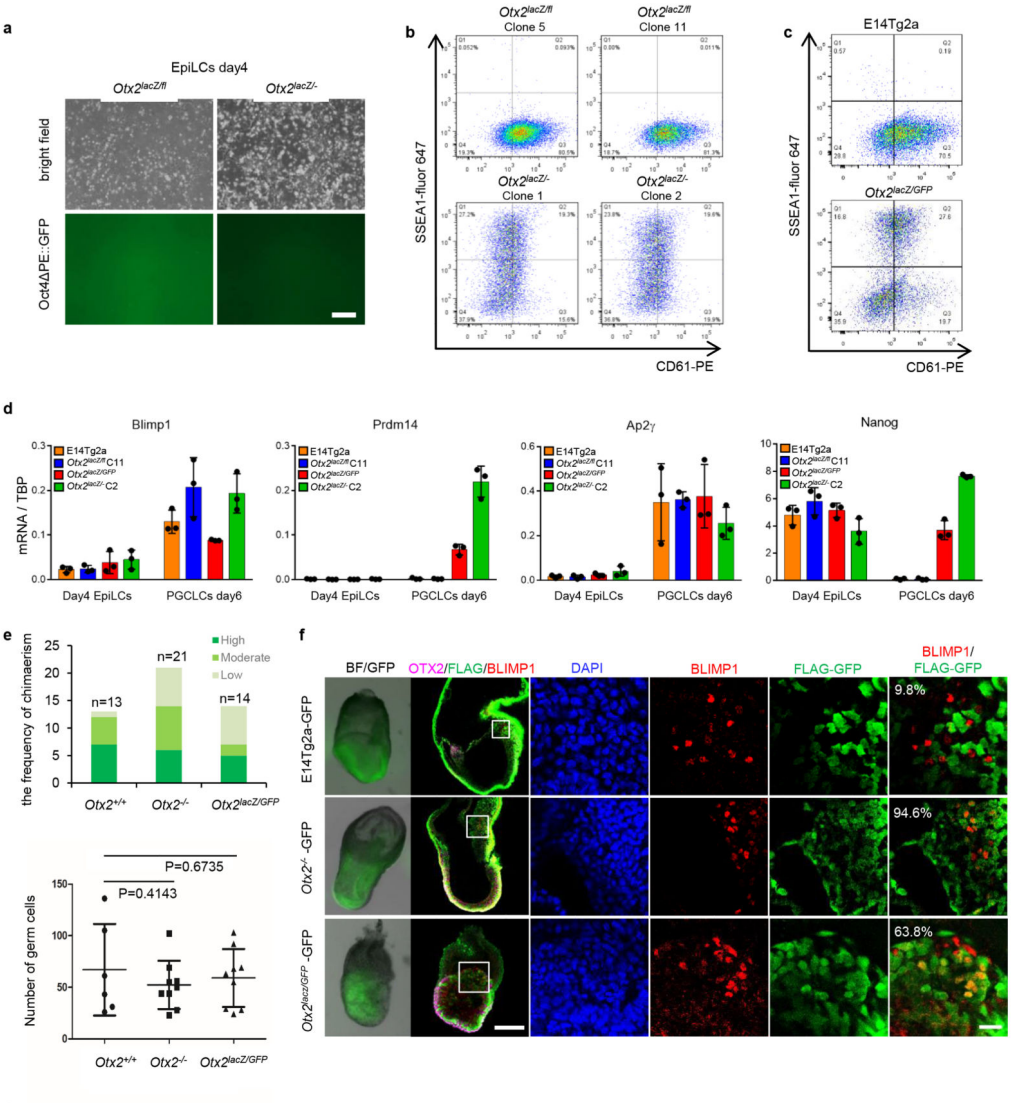

g

Cell lines	Embryos Transferred	No. of Embryos	No. of Chimaeras (% embryos)	No. for analysis
E14Tg2a-GFP	68	14	13 (92.8%)	6
Otx2$^{-/-}$ -GFP	86	33	21 (63.6%)	9
Otx2$^{lacZ/GFP}$ -GFP	57	18	14 (77.8%)	9

Extended Data Figure 9. OTX2 safeguards somatic lineages.

a. Representative morphologies and Oct4ΔPE::GFP expression of EpiSCs after 1 passage from EpiLCs (n=3 for 1 clone of each genotype). Bar; 200μm.

b, c. Flow cytometry analysis for surface expression of SSEA1 and CD61 at day 6 of PGCLC differentiation, initiated from EpiSCs after 1 passage from EpiLCs. For panel b, One experiment for c5 and c1 and 6 biologically independent replicates for C11 and C2; for panel c, n= 6 biologically independent replicates.

Europe PMC Funders Author Manuscripts

d. Quantitative transcript analysis of PGC TFs in the indicated cell lines. Expression levels are normalised to TBP; Values are means±SD, n= 3 biologically independent replicates., each dot represents the value from one experiment.

e. Comparison of the frequency of degree of chimaerism (top) and the germ cell numbers (bottom, centre lines and error bars represents means±SD.) in E7.5 chimaeric embryos formed using wildtype or Otx2-null ESCs. P value (two-tailed unpaired T-test, 0.95 confidence intervals) is indicated. High, > 70%; Moderate, 30 - 70%; Low, < 30%.

f. Bright field and representative images of E7.5 chimaeric embryos formed by wild-type host embryos and GFP labelled *Otx2*$^{+/+}$ (n=6), *Otx2*$^{-/-}$ (n=9) or *Otx2*$^{lacZ/GFP}$ (n=9) ESCs assessed for GFP and BLIMP1/SOX2 expression, with magnified images of the proximal posterior regions. The proportion of BLIMP1-positive cells expressing GFP in the embryos is indicated. Bar, 100μm (left) and 20μm.

g. Summary of embryo aggregations.

Europe PMC Funders Author Manuscripts

Europe PMC Funders Author Manuscripts

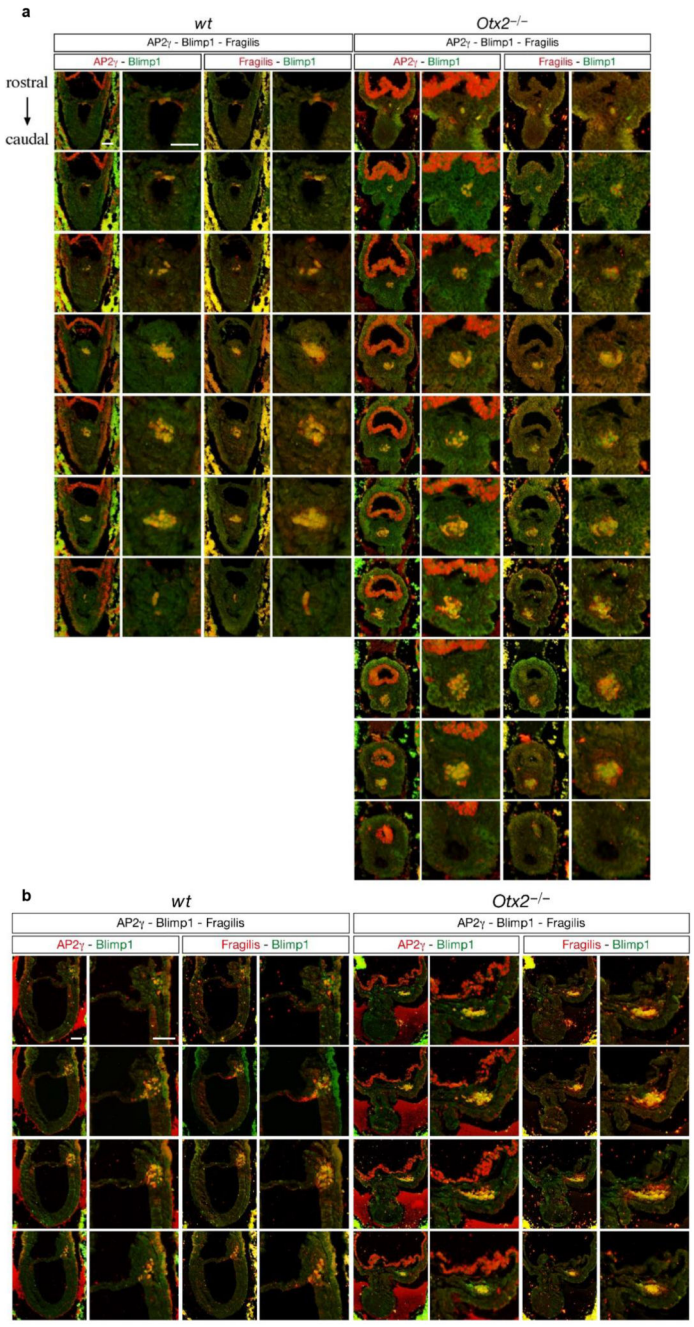

Extended Data Figure 10. *Otx2*-null embryos exhibit increased number of PGCs.

a, **b.** Frontal-coronal **(a)** and sagittal **(b)** sections of wild type and *Otx2*$^{-/-}$ E7.5 embryos stained with Blimp1, AP2γ and Fragilis to detect PGCs. All sequential sections spanning the PGCLCs niche are shown. Bar; 50μm. The experiments were repeated in 4 wt and 3 Otx2KO embryos.

Supplementary Material

Refer to Web version on PubMed Central for supplementary material.

Acknowledgments

We thank Val Wilson and Donal O'Carroll for comments on the manuscript, Val Wilson for help with embryo staging, Nick Mullin for pre-mRNA analyses, Pedro Moreira for help with embryo transfer, the CRM animal house staff for husbandry, Fiona Rossi and Claire Cryer for FACS and Bertrand Vernay for confocal assistance. This research was funded by the Medical and the Biotechnological and Biological Sciences Research Councils of the UK (IC), by a PRIN project from MIUR (AS) and by the Qilu Young Scholars Program of Shandong University (DY).

References

1. Ohinata Y, et al. A signaling principle for the specification of the germ cell lineage in mice. Cell. 2009; 137:571–584. DOI: 10.1016/j.cell.2009.03.014 [PubMed: 19410550]
2. Lawson KA, et al. Bmp4 is required for the generation of primordial germ cells in the mouse embryo. Genes & development. 1999; 13:424–436. [PubMed: 10049358]
3. Ohinata Y, et al. Blimp1 is a critical determinant of the germ cell lineage in mice. Nature. 2005; 436:207–213. DOI: 10.1038/nature03813 [PubMed: 15937476]
4. Vincent SD, et al. The zinc finger transcriptional repressor Blimp1/Prdm1 is dispensable for early axis formation but is required for specification of primordial germ cells in the mouse. Development. 2005; 132:1315–1325. DOI: 10.1242/dev.01711 [PubMed: 15750184]
5. Yamaji M, et al. Critical function of Prdm14 for the establishment of the germ cell lineage in mice. Nature genetics. 2008; 40:1016–1022. DOI: 10.1038/ng.186 [PubMed: 18622394]
6. Weber S, et al. Critical function of AP-2 gamma/TCFAP2C in mouse embryonic germ cell maintenance. Biology of reproduction. 2010; 82:214–223. DOI: 10.1095/biolreprod.109.078717 [PubMed: 19776388]
7. Johnson AD, Alberio R. Primordial germ cells: the first cell lineage or the last cells standing? Development. 2015; 142:2730–2739. DOI: 10.1242/dev.113993 [PubMed: 26286941]
8. Extavour CG, Akam M. Mechanisms of germ cell specification across the metazoans: epigenesis and preformation. Development. 2003; 130:5869–5884. DOI: 10.1242/dev.00804 [PubMed: 14597570]
9. McLaren A. Primordial germ cells in the mouse. Developmental biology. 2003; 262:1–15. [PubMed: 14512014]
10. Surani MA, Hayashi K, Hajkova P. Genetic and epigenetic regulators of pluripotency. Cell. 2007; 128:747–762. DOI: 10.1016/j.cell.2007.02.010 [PubMed: 17320511]
11. Saitou M, Yamaji M. Primordial germ cells in mice. Cold Spring Harbor perspectives in biology. 2012; 4doi: 10.1101/cshperspect.a008375
12. Hayashi K, Ohta H, Kurimoto K, Aramaki S, Saitou M. Reconstitution of the mouse germ cell specification pathway in culture by pluripotent stem cells. Cell. 2011; 146:519–532. DOI: 10.1016/j.cell.2011.06.052 [PubMed: 21820164]
13. Buecker C, et al. Reorganization of enhancer patterns in transition from naive to primed pluripotency. Cell stem cell. 2014; 14:838–853. DOI: 10.1016/j.stem.2014.04.003 [PubMed: 24905168]
14. Yang SH, et al. Otx2 and Oct4 drive early enhancer activation during embryonic stem cell transition from naive pluripotency. Cell reports. 2014; 7:1968–1981. DOI: 10.1016/j.celrep.2014.05.037 [PubMed: 24931607]
15. Acampora D, et al. Forebrain and midbrain regions are deleted in Otx2-/- mutants due to a defective anterior neuroectoderm specification during gastrulation. Development. 1995; 121:3279–3290. [PubMed: 7588062]
16. Ang SL, et al. A targeted mouse Otx2 mutation leads to severe defects in gastrulation and formation of axial mesoderm and to deletion of rostral brain. Development. 1996; 122:243–252. [PubMed: 8565836]
17. Acampora D, Di Giovannantonio LG, Simeone A. Otx2 is an intrinsic determinant of the embryonic stem cell state and is required for transition to a stable epiblast stem cell condition. Development. 2013; 140:43–55. DOI: 10.1242/dev.085290 [PubMed: 23154415]

Europe PMC Funders Author Manuscripts

18. Acampora D, et al. Functional Antagonism between OTX2 and NANOG Specifies a Spectrum of Heterogeneous Identities in Embryonic Stem Cells. Stem cell reports. 2017; 9:1642–1659. DOI: 10.1016/j.stemcr.2017.09.019 [PubMed: 29056334]
19. Nakaki F, et al. Induction of mouse germ-cell fate by transcription factors in vitro. Nature. 2013; 501:222–226. DOI: 10.1038/nature12417 [PubMed: 23913270]
20. Murakami K, et al. NANOG alone induces germ cells in primed epiblast in vitro by activation of enhancers. Nature. 2016; 529:403–407. DOI: 10.1038/nature16480 [PubMed: 26751055]
21. Magnusdottir E, et al. A tripartite transcription factor network regulates primordial germ cell specification in mice. Nature cell biology. 2013; 15:905–915. DOI: 10.1038/ncb2798 [PubMed: 23851488]
22. Smith A. Formative pluripotency: the executive phase in a developmental continuum. Development. 2017; 144:365–373. DOI: 10.1242/dev.142679 [PubMed: 28143843]
23. Gunesdogan U, Surani MA. Developmental Competence for Primordial Germ Cell Fate. Current topics in developmental biology. 2016; 117:471–496. DOI: 10.1016/bs.ctdb.2015.11.007 [PubMed: 26969996]
24. Saitou M, Barton SC, Surani MA. A molecular programme for the specification of germ cell fate in mice. Nature. 2002; 418:293–300. DOI: 10.1038/nature00927 [PubMed: 12124616]
25. Yoshimizu T, et al. Germline-specific expression of the Oct-4/green fluorescent protein (GFP) transgene in mice. Development, growth & differentiation. 1999; 41:675–684.
26. Zhang M, et al. Esrrb Complementation Rescues Development of Nanog-Null Germ Cells. Cell reports. 2018; 22:332–339. DOI: 10.1016/j.celrep.2017.12.060 [PubMed: 29320730]
27. Aramaki S, et al. A mesodermal factor, T, specifies mouse germ cell fate by directly activating germline determinants. Developmental cell. 2013; 27:516–529. DOI: 10.1016/j.devcel.2013.11.001 [PubMed: 24331926]
28. Ben-Haim N, et al. The nodal precursor acting via activin receptors induces mesoderm by maintaining a source of its convertases and BMP4. Developmental cell. 2006; 11:313–323. DOI: 10.1016/j.devcel.2006.07.005 [PubMed: 16950123]
29. John SA, Garrett-Sinha LA. Blimp1: a conserved transcriptional repressor critical for differentiation of many tissues. Experimental cell research. 2009; 315:1077–1084. DOI: 10.1016/j.yexcr.2008.11.015 [PubMed: 19073176]
30. Kurimoto K, et al. Complex genome-wide transcription dynamics orchestrated by Blimp1 for the specification of the germ cell lineage in mice. Genes & development. 2008; 22:1617–1635. DOI: 10.1101/gad.1649908 [PubMed: 18559478]
31. Hemmati-Brivanlou A, Melton D. Vertebrate embryonic cells will become nerve cells unless told otherwise. Cell. 1997; 88:13–17. [PubMed: 9019398]
32. Levine AJ, Brivanlou AH. Proposal of a model of mammalian neural induction. Developmental biology. 2007; 308:247–256. DOI: 10.1016/j.ydbio.2007.05.036 [PubMed: 17585896]
33. Smith AG. Culture and differentiation of embryonic stem cells. Journal of tissue culture methods. 1991; 13:89–94. DOI: 10.1007/bf01666137
34. Zhang M, et al. Esrrb Complementation Rescues Development of Nanog -Null Germ Cells. Cell Reports. 2018; 22:332–339. DOI: 10.1016/j.celrep.2017.12.060 [PubMed: 29320730]
35. Hayashi K, Saitou M. Generation of eggs from mouse embryonic stem cells and induced pluripotent stem cells. Nat Protoc. 2013; 8:1513–1524. DOI: 10.1038/nprot.2013.090 [PubMed: 23845963]
36. Lamprecht MR, Sabatini DM, Carpenter AE. CellProfiler: free, versatile software for automated biological image analysis. Biotechniques. 2007; 42:71–75. [PubMed: 17269487]
37. Gagliardi A, et al. A direct physical interaction between Nanog and Sox2 regulates embryonic stem cell self-renewal. The EMBO journal. 2013; 32:2231–2247. DOI: 10.1038/emboj.2013.161 [PubMed: 23892456]
38. Schmittgen TD, Livak KJ. Analyzing real-time PCR data by the comparative C(T) method. Nat Protoc. 2008; 3:1101–1108. [PubMed: 18546601]
39. Bronson RA, McLaren A. Transfer to the mouse oviduct of eggs with and without the zona pellucida. Journal of reproduction and fertility. 1970; 22:129–137. [PubMed: 5421101]

Europe PMC Funders Author Manuscripts

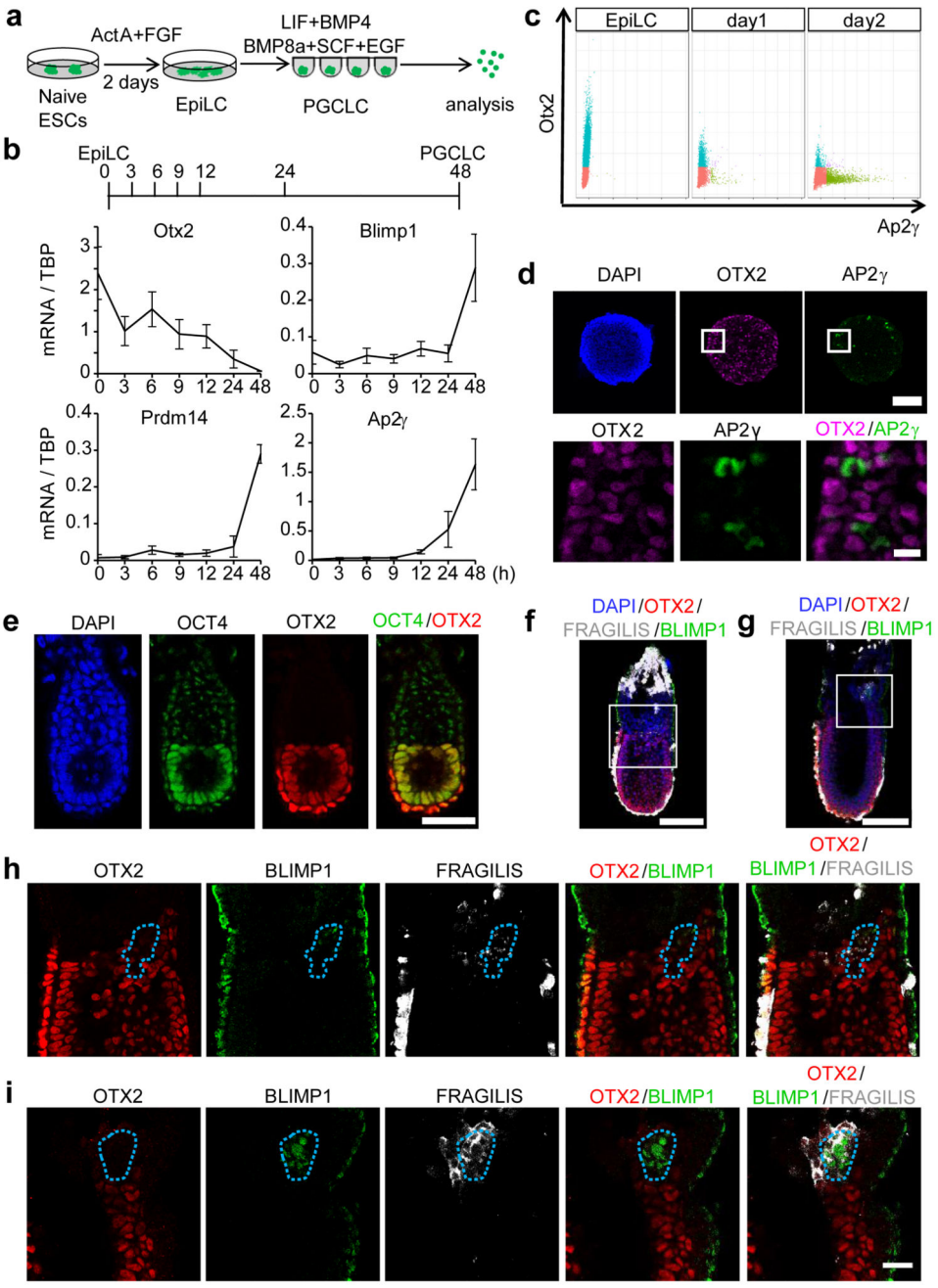

Figure 1. Otx2 expression is down-regulated prior to expression of PGC TFs.

a. Scheme for PGCLC differentiation.

b. Top, scheme illustrating the time-points (hours) during PGCLC differentiation when mRNAs were analysed. Bottom, Q-RT-PCR of Otx2 and PGC TFs in E14Tg2a ESCs. Expression levels are normalised to TBP; h, hours; Values are means±SD, n= 3 biologically independent replicates.

c. Single cell quantification of immunofluorescence for Otx2 and Ap2γ in cytospin preparations of EpiLCs and cell aggregates at day 1 and day 2 of PGCLC induction. 2 biologically independent replicates were performed.

d. Whole mount immunofluorescence of E14Tg2a aggregates after 1 day of PGCLC differentiation. n=3. Scale bar, 50μm (top) and 10μm (bottom)

e-g. Representative confocal images of whole mount staining of embryos at pre-streak (e, n=4), early streak (f, n=3) and late streak (g, n=3) stages. Bar = 40μm (e), 100μm (f, g).

h-i. Magnified image of the regions highlighted in (**f**) and (**g**) respectively. OTX2-negative cells expressing BLIMP1 and FRAGILIS are outlined (g, h). Bar = 20μm.

Europe PMC Funders Author Manuscripts

Europe PMC Funders Author Manuscripts

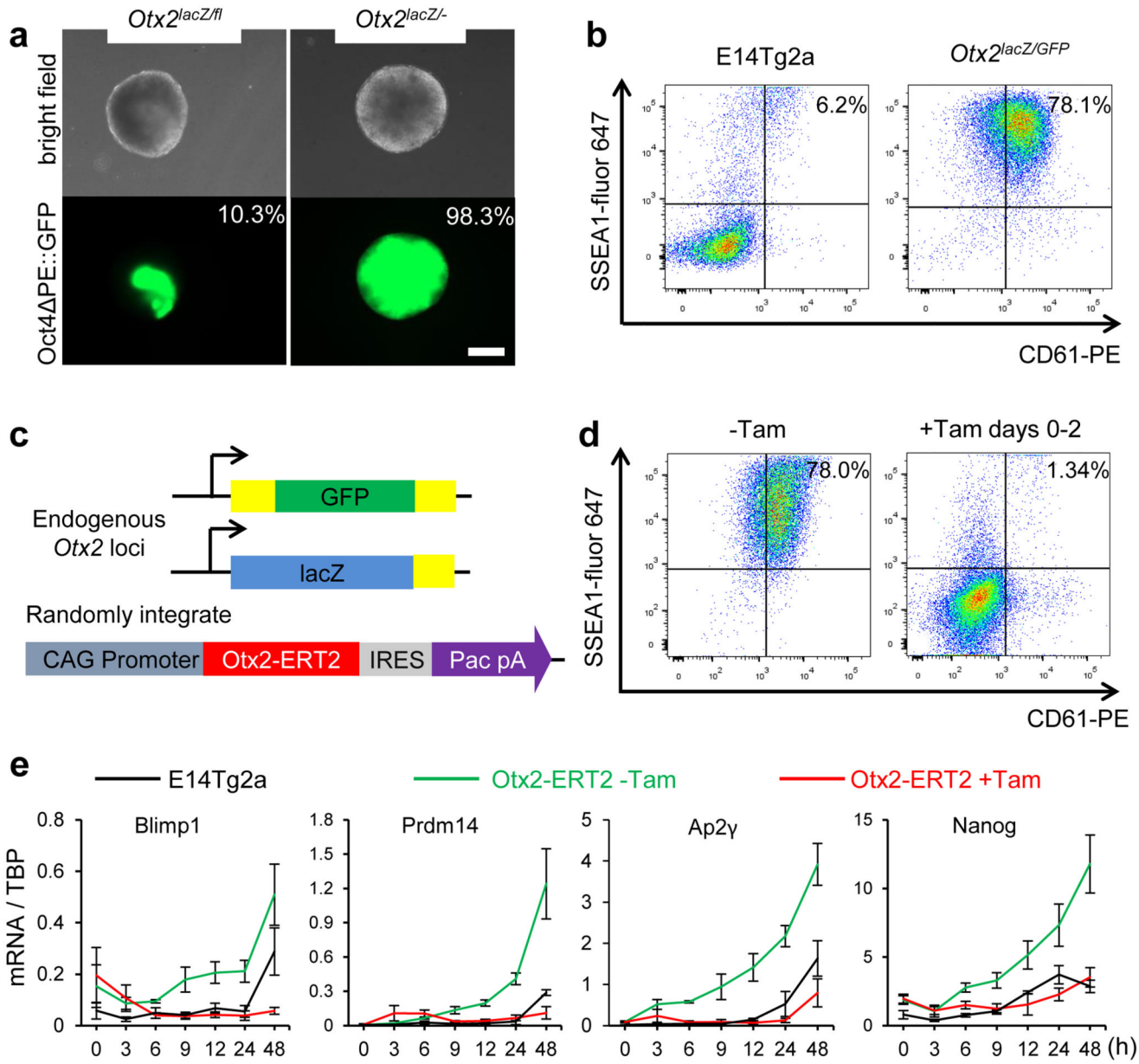

Figure 2. *Otx2*$^{-/-}$ EpiLCs have an enhanced propensity to differentiate into PGCLCs.

a. Representative morphologies and Oct4ΔPE::GFP expression in aggregates at day 4 of PGCLC differentiation in the presence of cytokines. Percentages indicate GFP-positive cells; n=9. Bar = 200μm.

b. E14Tg2a and *Otx2*$^{-/-}$ cells were assessed by flow cytometry for surface expression of SSEA1 and CD61 at days 6 of PGCLC differentiation; (n=12).

c. Diagram of the tamoxifen inducible Otx2 cell line, carrying an Otx2-ER^{T2} fusion protein transgene and replacements of endogenous *Otx2* alleles by *GFP* or *LacZ*.

d. *Otx2*$^{lacZ/GFP}$::Otx2ER^{T2} cells were assessed by flow cytometry for surface expression of SSEA1 and CD61 at day 6 of PGCLC differentiation, either without Tamoxifen or with Tamoxifen from days 0-2, n= 4 biologically independent replicates.

e. Q-RT-PCR of PGC TFs. Expression levels are normalised to TBP; h, hours; Values are means±SD, n= 3 biologically independent replicates.

Europe PMC Funders Author Manuscripts

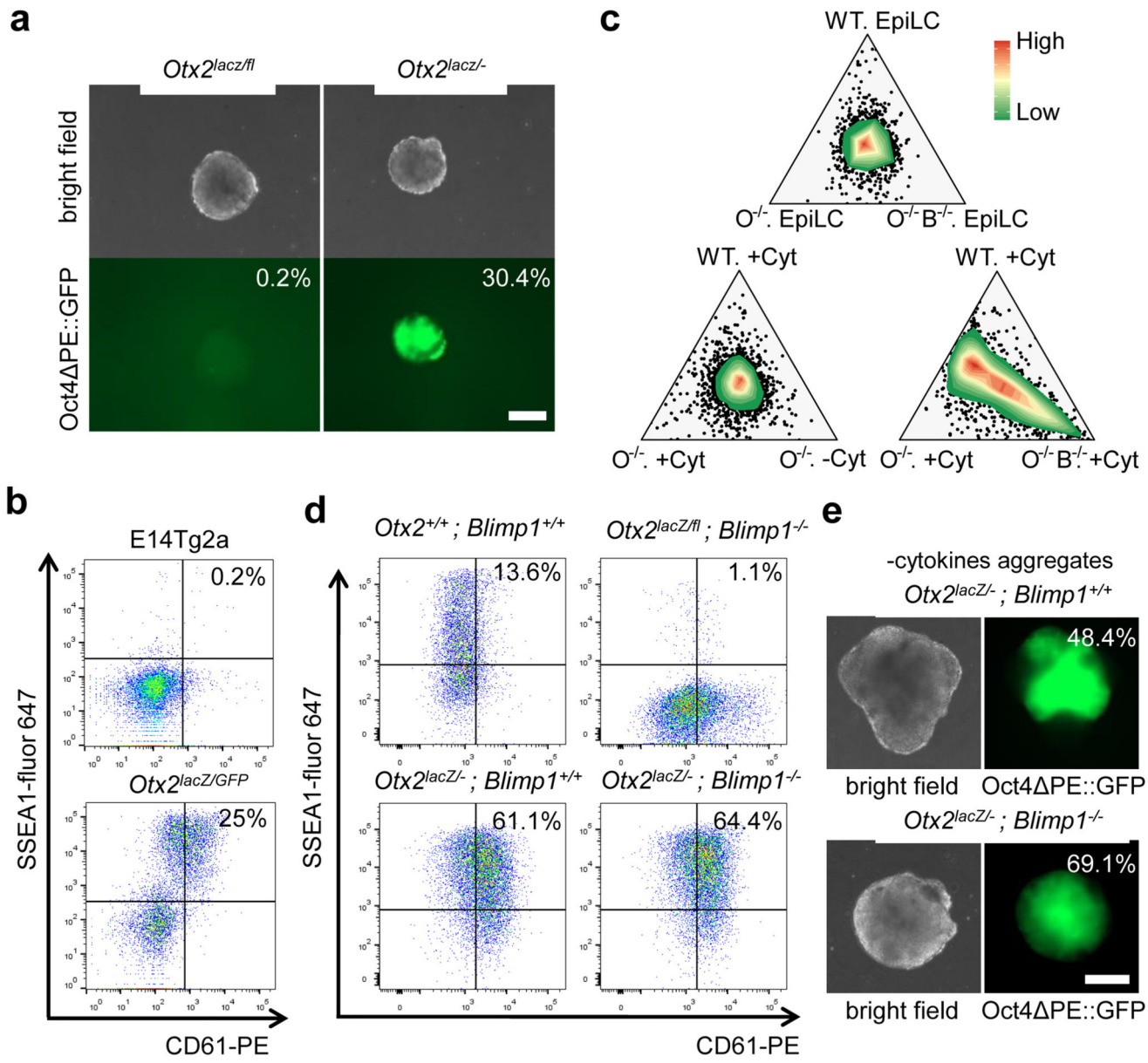

Figure 3. *Otx2*-null cells can access the germline independently of cytokines and Blimp1.

a. Representative morphologies and Oct4ΔPE::GFP expression in aggregates at day 4 of PGCLC differentiation without cytokines. Percentages indicate GFP-positive cells; (n= 7). Bar = 200μm.

b. E14Tg2a and *Otx2*$^{-/-}$ cells were assessed by flow cytometry for surface expression of SSEA1 and CD61 at day 6 of differentiation in the absence of PGCLC cytokines; (n=9).

c. Ternary plot analysis (microarray data from 3 biologically independent replicates under 7 different conditions) comparing transcriptomes of EpiLCs (top) or day6 PGCLCs (bottom). Circles represent probes, with colour indicating the probe density. Differentiations performed in the presence or absence of cytokines are indicated (+/-Cyt). WT, E14Tg2a; O$^{-/-}$, *Otx2*$^{lacZ/GFP}$; O$^{-/-}$ B$^{-/-}$, *Otx2*$^{lacZ/GFP}$ *Blimp1*$^{-/-}$.

d. Cells of the indicated genotypes were assessed by flow cytometry for surface expression of SSEA1 and CD61 at day 6 of PGCLC differentiation; (n=2 for 1 clone of each genotype). Two further clones of each genotype are shown in Extended Data Figure 6.

e. Cytokine-free PGCLC differentiation. Representative morphologies and Oct4ΔPE::GFP expression of aggregates at day 6. Percentages indicate GFP-positive cells; (n=2 for 1 clone of each genotype). Bar = 200μm.

Europe PMC Funders Author Manuscripts

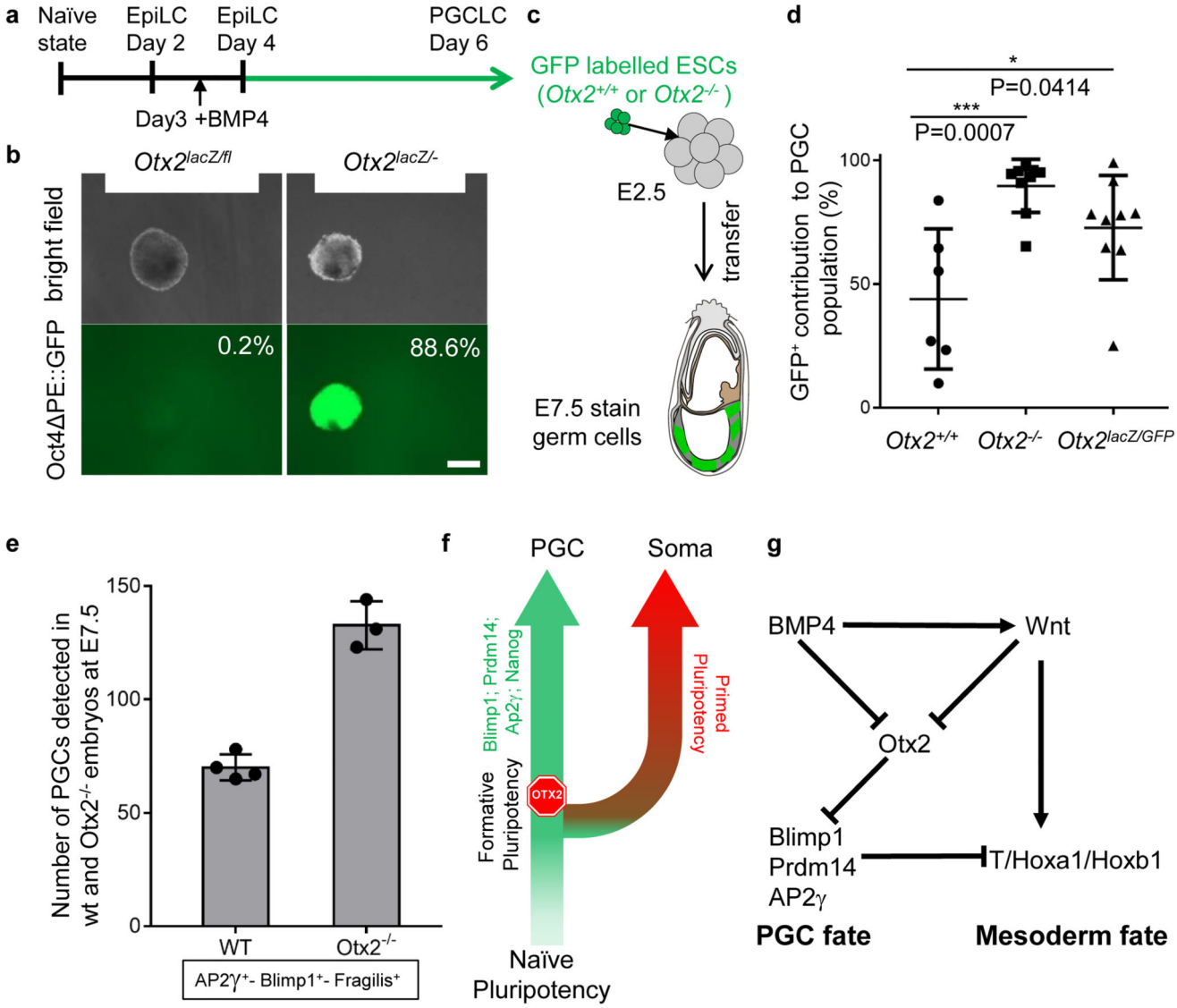

Figure 4. *Otx2*$^{-/-}$ ESCs contribute to the germline at an enhanced rate in vivo.

a. Scheme for PGCLC differentiation, initiated from day 4 EpiLCs obtained after 1 passage from EpiLCs.

b. Representative morphologies and Oct4ΔPE::GFP expression from aggregates at day 6 of PGCLC differentiation from EpiLCs day4 (n=3 for 1 clone of each genotype). Bar = 200μm.

c. Scheme for generating chimaeras of GFP labelled *Otx2*$^{+/+}$ or *Otx2*$^{-/-}$ ESCs with wildtype host embryos.

d. Comparison of the percentage contribution of GFP labelled wildtype (n=6) or *Otx2*-null ESCs (genotypes indicated, n=9 for each) to the PGC population in E7.5 chimaeric embryos. Each dot represents the percentage from one chimaera, centre lines and error bars represents means±SD. P value (two-sided unpaired T-test, 0.95 confidence intervals) is indicated. GFP positive cells were counted within the PGC population marked with BLIMP1 or SOX2 in each embryo.

Europe PMC Funders Author Manuscripts

e. Comparison of PGCs number in wild-type (n= 4) and *Otx2*$^{-/-}$ (n= 3) E7.5 embryos. PGCs were identified with Blimp1, AP2γ and Fragilis. Values= means ± SD.
f. Model indicating the point of operation of OTX2 during germline-soma segregation.
g. A scheme illustrating the regulatory relationships upstream and downstream of *Otx2* during germline segregation.

Europe PMC Funders Author Manuscripts